



Hochschule für Angewandte Wissenschaften Hamburg  
*Hamburg University of Applied Sciences*

## **Master Thesis**

**Departement Fahrzeugtechnik und Flugzeugbau**

### **Conceptual Design of Wings and Tailplanes – Methods, Statistics, Tool Setup**

**Steven Coene**

**30. June 2008**



Hochschule für Angewandte Wissenschaften Hamburg  
Fakultät Technik und Informatik  
Department Fahrzeugtechnik + Flugzeugbau  
Berliner Tor 9  
20099 Hamburg

in cooperation with:

KHBO  
Katholieke hogeschool Brugge - Oostende  
Campus Oostende  
Zeedijk 101, B-8400 Oostende

Author: Steven Coene  
Submission date: 30.06.08

1. Examiner: Prof. Dr.-Ing. Dieter Scholz
2. Examiner: Dipl.-Ing. Kolja Seeckt

## Abstract

This Master Thesis deals with the tool setup for conceptual design of the wing and the empennage of subsonic civil transport aircraft, based on minimal input data. The tool is set up in Microsoft excel but is designed to work also in Openoffice. This thesis deals with some theoretical explanation of the design steps and guidelines given by different authors, in order to achieve the minimal input data objective. These guidelines were integrated into an excel spread sheet where the main wing and empennage geometry parameters (e.g. taper ratio, sweep angle, thickness ratio...) can be defined. Based on these input parameters, a first geometrical description of the wing and empennage is calculated along with many derived parameters (e.g. mean aerodynamic chord, leading edge sweep angle, wing lift gradient, incidence angle ...) which are useful in later phases in the design. The tool also includes top and side views of the wing and empennage and is made as user-friendly as possible, while still maintaining the adjustability of the design model. For example there are diagrams included which show one design parameter set out to another according to the different guidelines. In these diagrams the design point is also added to show the user where the current model is situated.



## DEPARTMENT FAHRZEUGTECHNIK UND FLUGZEUGBAU

# Conceptual Design of Wings and Tailplanes – Methods, Statistics, Tool Setup

Task for a *Master Thesis* at KHBO

## Background

This master thesis is part of the aircraft design research project “Green Freighter” (<http://GF.ProfScholz.de>). In this project the tool PrADO “Preliminary Aircraft Design and Optimization program” is used to investigate and optimize different aircraft configurations which requires an extensive input file.

## Task

The student shall create a tool to support the conceptual design of aircraft wings and tailplanes. Based on a minimum of input data, wings and tailplanes shall be defined in as much detail as required in conceptual design. In addition, the generated data shall be available in a format that facilitates the generation of a PrADO input file. The thesis shall include

- the research of elements towards a conceptual design of aircraft wings and tailplanes,
- the combination of the conceptual design elements with own statistics towards a comprehensive conceptual layout process for wings and tailplanes,
- the programming of an easy-to-use tool for conceptual wing and tailplane design based on MS Excel, the programming of an interface to generate sections of the PrADO input file required for the definition of wings and tailplanes.

This Master Thesis is related to a second Master Thesis “Conceptual Design of Fuselages, Cabins and Landing Gears – Methods, Statistics, Tool Setup”. Both theses shall apply the same layout principles, programming styles and styles defined for the user interface.

The report has to be written according to German or international standards on report writing!

## **Declaration**

This Master Thesis is entirely my own work. Where use has been made of the work of others, it has been fully acknowledged and referenced.

June 30, 2008

**Date**

**Signature**

# Contents

	Page
Abstract .....	3
Declaration .....	5
List of Figures.....	8
List of Tables.....	9
List of symbols .....	10
Greek symbols .....	11
List of indices .....	12
List of Abbreviations.....	12
<b>1 Introduction .....</b>	<b>13</b>
1.1 Motivation .....	13
1.2 Objectives.....	13
1.3 Literature overview .....	14
1.4 Terms and definitions.....	15
1.5 Report structure .....	18
<b>2 Conceptual design of wings .....</b>	<b>19</b>
2.1 Design requirements.....	20
2.1.1 Cruise requirements.....	20
2.1.2 Take off and landing requirements.....	21
2.1.3 Taxi and terminal requirements.....	21
2.1.4 Operation.....	21
2.2 Input parameters from earlier design phases.....	22
2.2.1 Maximum take off mass and wing loading .....	23
2.2.2 Fuselage diameter.....	23
2.2.3 Aspect ratio.....	23
2.2.4 Cruise Mach number $M_c$ .....	23
2.2.5 Cruise lift coefficient $C_{L,C}$ .....	23
2.2.6 General wing-fuselage arrangement.....	24
2.3 Thickness to chord ratio and sweep angle.....	24
2.3.1 Low subsonic.....	24
2.3.2 High subsonic .....	26
2.3.3 Thickness distribution .....	29
2.3.4 Sweep angle geometry calculations .....	30
2.4 Airfoil section.....	32
2.4.1 NACA airfoils .....	33
2.4.2 Airfoil selection.....	36
2.4.3 Airfoil properties .....	38
2.5 Lift distribution.....	38
2.5.1 Wing twist .....	39

2.5.2	Taper ratio .....	39
2.5.3	Double tapered wing .....	41
2.6	Aerodynamic center of the wing .....	44
2.7	Incidence angle.....	46
2.8	Dihedral angle .....	47
2.9	Wing control surfaces – ailerons .....	49
2.9.1	Different types of ailerons .....	49
2.9.2	Low speed aileron surface sizing .....	50
2.9.3	Aileron geometry.....	51
2.9.4	High speed aileron surface sizing.....	52
2.10	Lift predictions of the wing .....	54
2.10.1	Wing lift gradient. ....	54
2.10.2	Maximum clean wing lift coefficient .....	55
2.10.3	Maximum wing lift coefficient with high lift devices.....	55
2.11	High lift devices .....	56
2.12	Fuel tank estimation .....	59
3	Conceptual design of the empennage.....	<b>60</b>
3.1	General empennage configurations .....	61
3.2	Surface size of the empennage .....	61
3.3	Geometry selection.....	67
3.3.1	Wing shape .....	67
3.3.2	Sweep angle and thickness to chord ratio .....	68
3.4	Airfoil selection.....	69
3.5	Empennage control surfaces - elevator and rudder .....	71
3.5.1	Elevator .....	71
3.5.2	Rudder .....	72
3.6	Tail placement .....	74
3.6.1	Engine slipstream .....	74
3.6.2	Stall control .....	75
3.6.3	Spin recovery.....	77
	<b>Conclusion.....</b>	<b>80</b>
	<b>Final remarks .....</b>	<b>81</b>
	Acknowledgements.....	82
	References.....	83
	Appendix A Source code of airfoil input macro.....	84

## List of figures

<b>Figure 1.1</b>	Wing top view and geometry definitions.....	15
<b>Figure 1.2</b>	Reference area $S_{ref}$ definitions of Boeing and Airbus .....	16
<b>Figure 1.3</b>	Axes of an aircraft .....	17
<b>Figure 1.4</b>	Critical Mach number and Drag divergence Mach number .....	18
<b>Figure 2.1</b>	Wing with all major parameters defined. ....	19
<b>Figure 2.2</b>	Typical climb schedule .....	20
<b>Figure 2.3</b>	Design requirements of a wing .....	22
<b>Figure 2.4</b>	Preliminary sizing input data as implemented in the tool. ....	22
<b>Figure 2.5</b>	Thickness to chord suggestions for low subsonic Mach numbers .....	25
<b>Figure 2.6</b>	Leading edge sweep suggestion .....	26
<b>Figure 2.7</b>	Different guidelines of thickness to chord suggestions.....	27
<b>Figure 2.8</b>	2-D and 3-D flow characteristics over the wing.....	28
<b>Figure 2.9</b>	Thickness to chord distribution .....	29
<b>Figure 2.10</b>	Sweep angle and thickness selection as implemented in the tool .....	32
<b>Figure 2.11</b>	NACA 2415 airfoil .....	33
<b>Figure 2.12</b>	NACA 23015 airfoil .....	34
<b>Figure 2.13</b>	NACA 65 <sub>2</sub> -415 airfoil .....	35
<b>Figure 2.14</b>	Screenshot of airfoil data spread sheet. ....	36
<b>Figure 2.15</b>	Airfoil selection as implemented in the tool.....	37
<b>Figure 2.16</b>	Difference between aerodynamic and weight optimal lift distribution .....	38
<b>Figure 2.17</b>	Lift distribution for various taper ratios .....	39
<b>Figure 2.18</b>	Taper ratios of straight, swept and delta wings .....	40
<b>Figure 2.19</b>	Section lift distribution on straight wings with various taper ratios.....	41
<b>Figure 2.20</b>	Graph with various taper ratio suggestions as included in the tool.....	43
<b>Figure 2.21</b>	The thickness distribution as implemented in the tool. ....	44
<b>Figure 2.22</b>	Cruise wing lift coefficient range during cruise flight. ....	46
<b>Figure 2.23</b>	Layout requirements for dihedral angle.....	47
<b>Figure 2.24</b>	wing twist, incidence angle and dihedral angle.....	49
<b>Figure 2.25</b>	Aileron chord and span guidelines .....	50
<b>Figure 2.26</b>	Aileron design as implemented in the tool .....	53
<b>Figure 2.27</b>	Different types of high lift devices .....	56
<b>Figure 2.28</b>	Definition of flapped wing area.....	58
<b>Figure 2.29</b>	High lift device selection in the tool.....	58
<b>Figure 2.30</b>	Fuel tank volume estimation in the tool. ....	59
<b>Figure 3.1</b>	Horizontal and vertical tail as described in the tool. ....	60
<b>Figure 3.2</b>	Different empennage configurations .....	61
<b>Figure 3.3</b>	Definition of empennage surfaces and lever arms.....	63
<b>Figure 3.4</b>	Input data, general arrangement and surface sizing of the empennage.....	66
<b>Figure 3.5</b>	Geometry selection of the horizontal tail .....	70



<b>Figure 3.6</b>	Elevator geometry selection integrated in tool.....	72
<b>Figure 3.7</b>	Rudder geometry selection as integrated in the tool .....	74
<b>Figure 3.8</b>	Position of the horizontal tail guidelines .....	75
<b>Figure 3.9</b>	Position of the horizontal tail guidelines as implemented in the Tool .....	77
<b>Figure 3.10</b>	Tail geometry for spin recovery .....	78
<b>Figure 3.11</b>	Horizontal tail wake simulated in the tool.....	79

## List of tables

<b>Table 2.1</b>	Typical airliner wing span limits.....	21
<b>Table 2.2</b>	km Factors in thickness equations .....	29
<b>Table 2.3</b>	Kink ratios for different aircraft types.....	42
<b>Table 2.4</b>	Dihedral guidelines.....	48
<b>Table 2.5</b>	Dihedral guidelines.....	48
<b>Table 2.6</b>	Dihedral guidelines as used in the tool by.....	48
<b>Table 2.7</b>	Dihedral guidelines as used in the tool by.....	48
<b>Table 2.8</b>	Aileron guidelines.....	51
<b>Table 2.9</b>	High lift device efficiency .....	57
<b>Table 3.1</b>	Tail volume coefficients .....	64
<b>Table 3.2</b>	First lever arm estimation .....	64
<b>Table 3.3</b>	Equivalent Tail volume coefficients for different configurations .....	65
<b>Table 3.4</b>	Horizontal tail geometry guidelines .....	67
<b>Table 3.5</b>	Vertical tail geometry guidelines.....	67
<b>Table 3.6</b>	Empennage guidelines.....	67
<b>Table 3.7</b>	Elevator chord and span guidelines.....	71
<b>Table 3.8</b>	Rudder chord and span guidelines.....	73

## List of symbols

$A$	Wing Aspect ratio
$b$	Wing span
$b_A$	Total aileron span
$b_A/b$	Total aileron span ratio
$b_{A,H}$	total high speed aileron
$b_{A,H}/b$	Total high speed aileron span ratio
$b_E$	Total elevator span
$b_H$	Total horizontal tail span
$b_R$	rudder span
$b_V$	vertical tail span
$c$	Chord length
$c_A/c$	Aileron chord ratio
$c_{A,H}/c$	High speed aileron chord ratio
$c_E/c$	Elevator chord ratio
$C_H$	Horizontal tail volume coefficient
$C_{L\alpha}$	Wing lift gradient, wing lift curve slope
$C_{L,c}$	design lift coefficient (cruise lift coefficient)
$C_{L,H}$	Horizontal tail cruise lift coefficient
$C_{L,L}$	Landing lift coefficient
$C_{L,TO}$	Take off lift coefficient
$C_{L,V}$	Vertical tail cruise lift coefficient
$C_V$	Vertical tail volume coefficient
$d_f$	Fuselage diameter
$F$	Fuselage lift factor
$i$	Wing incidence angle
$i_H$	Horizontal tail incidence angle
$k_{m,Torenbeek}$	technology standard of wing airfoil used in Torenbeek's equation of thickness
$k_{m,nonlinear}$	Technology standard of wing airfoil used in Non-linear regression equation of thickness
$k_{m,Torenbeek,H}$	Technology standard of horizontal tail airfoil used in Torenbeek's equation of thickness
$k_{m,Torenbeek,V}$	Technology standard of vertical tail airfoil used in Torenbeek's equation of thickness
$l_f$	Fuselage length
$l_H$	Horizontal tail lever arm around center of gravity
$l_H/c_{MAC}$	horizontal tail lever arm ratio
$l_V$	Vertical tail lever arm around center of gravity
$M_c$	Cruise Mach number
$M_{cr}$	Critical Mach number
$M_{DD}$	Drag divergence Mach number
$M_{DD,E}$	Empennage drag divergence Mach number

$M_{DD,eff}$	Effective drag divergence Mach number of wing
$M_{DD,eff,H}$	Effective drag divergence Mach number of horizontal tail
$M_{DD,eff,V}$	Effective drag divergence Mach number of vertical tail
$m_F$	Fuel mass calculated from wing geometry
$m_{FC}$	Fuel mass required from preliminary sizing
$m_{MTO}$	Maximum take off mass
$S$	Total wing area (= $S_{ref}$ )
$S/W$	Wing loading
$S_A$	Surface Area
$S_{ref}$	Wing reference area
$S_V$	Vertical tail area
$(t/c)$	Average wing thickness to chord ratio
$(t/c)_k$	Wing kink thickness to chord ratio
$(t/c)_r$	Wing root thickness to chord ratio
$(t/c)_t$	Wing tip thickness to chord ratio
$V_A$	Aileron volume coefficient
$V_F$	Total fuel tank volume
$Y$	semi-span location
$Z_r$	vertical position of the root chord of the wing
$Z_{r,H}$	vertical position of the root chord of the horizontal tail
$Z_{r,V}$	vertical position of root chord of vertical tail

## Greek symbols

$\alpha_{CL=0}$	zero lift angle of attack of the wing airfoil
$\Delta_{cl,LE}$	Section lift increase due to leading edge high lift devices
$\Delta_{cl,TE}$	Section lift increase due to Trailing edge high lift devices
$\Delta_{CL,LE}$	Wing lift increase due to leading edge high lift devices
$\Delta_{CL,TE}$	Wing lift increase due to trailing edge high lift devices
$\Delta_{IH}$	Shift backward of horizontal tail with respect to lever arm
$\Delta_{MDD}$	MDD-Mc definition
$\Delta_{ZH}$	Vertical distance between wing MAC and horizontal tail MAC
$\Delta_{ZH/cMAC}$	Vertical distance of horizontal tail MAC above wing MAC ratio
$\Gamma$	Wing dihedral angle
$\Gamma_H$	Horizontal tail dihedral angle
$\Gamma_V$	Vertical tail dihedral angle
$\varepsilon_t$	Total wing twist
$\varepsilon_{t,a}$	Aerodynamic wing twist
$\varepsilon_{t,g}$	Geometric wing twist
$\eta_l$	Lever arm ratio ( lever arm / fuselage length)

$\eta_k$	Kink ratio ( $Y_k/b$ )
$\rho_F$	Fuel density
$\lambda$	Taper ratio ( $c_t/c_r$ )
$\Lambda$	sweep angle
$\tau$	Wing tip-to-root relative thickness ratio $\left(\frac{t}{c}\right)_t / \left(\frac{t}{c}\right)_r$

## List of indices

(no indice)	Wing of aircraft
25	25% chord line in wing direction
50	50% chord line in wing direction
$A$	Aileron
$A,H$	High speed Aileron
$f$	Fuselage
$F$	Fuel
$H$	Horizontal tail
$i$	Wing inner trapezoid
$LE$	Leading edge
MAC	Mean aerodynamic chord
$o$	Wing outer trapezoid
$R$	Rudder
$r$	Root
$TE$	Trailing edge
$V$	Vertical tail
$W$	Wing of aircraft

## List of abbreviations

CG	Center of gravity
MAC	Mean aerodynamic chord
PrADO	Preliminary Aircraft Design and Optimization program
PreSTo	Preliminary Sizing Tool

# 1 Introduction

## 1.1 Motivation

Conceptual design can be done through calculations by hand with simple guideline equations containing different design constraints. Because of the iterative nature of the design process, many calculations by hand should be overdone again and again. Therefore it is useful to include the equations in an automated calculation process which recalculates all derived dimensions if an earlier designated dimension has to be changed.

This thesis focuses on the design of a tool for conceptual wing and empennage design and the following step after the preliminary sizing tool or shortly PreSTo.

This tool is also part of the “Green Freighter” project (<http://GF.ProfScholz.de>) in this project the tool PrADO “Preliminary Aircraft Design and Optimization program” is used to investigate and optimize different aircraft configurations, which requires an extensive input file. The second goal of the tool created here is to quickly generate these extensive PrADO input files.

The tool focuses on civil transport aircraft with conventional configuration, with high or low wing, at high and low subsonic speeds. It therefore includes business jets, regional turboprops and jet transport aircraft.

## 1.2 Objectives

The objective is to create a tool to support the conceptual design of aircraft wings and empennage. Based on a minimum of input data, wings and empennage shall be defined in as much detail as required in the conceptual design.

The student shall create a tool to support the conceptual design of aircraft wings and tailplanes. Based on a minimum of input data, wings and tailplanes shall be defined in as much detail as required in conceptual design. In addition, the generated data shall be available in a format that facilitates the generation of a PrADO input file.

The creation of the tool starts with the research of elements towards a conceptual design of aircraft wings and tailplanes and the combination of the conceptual design elements with own statistics towards a comprehensive conceptual layout process for wings and tailplanes.

This Master Thesis is related to a second Master Thesis “Conceptual Design of Fuselages,

Cabins and Landing Gears – Methods, Statistics, Tool Setup”. (Goderis 2008) Both theses have to apply the same layout and programming

### 1.3 Literature overview

Note that this literature overview is not complete; it gives only the books most referred to in this master thesis. This is also not entirely objective, because for the writing of this master thesis, only the conceptual design of wing and the empennage parts of the books were used.

- **Aircraft Design: A Conceptual Approach - Raymer 2006**

This book presents the entire conceptual design process of an aircraft, from requirements definition to initial sizing, configuration layout, analysis, sizing and trade studies. Everything is also elaborately and clearly explained, it is really a good basis for understanding the matters. In some cases the book does not always contains an actual value as guideline, but it is still a very good reference.

- **Airplane Design. Part II : Preliminary Configuration Design and Integration of the Propulsion System – Roskam 1989**

This book gives an elaborate description off all the design steps; it also gives a lot of data on existing aircraft. Sometimes things are explained not that good and general guidelines are a bit rare. The book also uses a lot of charts, which are not convenient to convert in an automated tool. It contains a huge amount of information and gives the design always very organized in steps so it is a good manual for a structured design.

- **Aircraft Conceptual Design Synthesis – Howe 2000**

This book is very good to get an actual initial value and the explanations are always clear and to the point. This book is really one of the better ones in just describing the things needed, but it is definitely not as elaborate as the two latter books. When starting with a “normal” design, this is a good starting point.

- **Synthesis of Subsonic Airplane Design – Torenbeek 1988**

This book gives a very clear insight in the “why” of certain design choices; it explains design in a scientific, theoretic way. It contains a lot of theoretical or empirical equations for finding different design parameters. A bit of a downside is that it is sometimes difficult to find what u actually need, because of the huge amount of explained things it contains. This book is a good start for really understanding the phenomena of flying.

## 1.4 Terms and definitions

### Design requirement

A technical requirement (range, payload, flight performance, etc.) which is imposed either by the customer or the aircraft manufacturer. When the design is ready, these requirements will have to be met.

### Design constraint

A design constraint can be chosen freely by the designer, but only in this way that the design requirements can be met when the aircraft is flying. This means that the designers freely can choose these parameters within a range where it is possible to satisfy the design requirements.

### Reference area $S$ or $S_{ref}$

The wing top view given in Figure 1.1 draws the right half of the aircraft wing, with a definition of the main wing parameters. The center line on the right side is the centerline of the aircraft. The wing area as drawn here is the reference area  $S_{ref}$  or short  $S$ . This is the arbitrary chosen area of the wing; during the design all the calculations will be done with this area as if it were the real wing area.

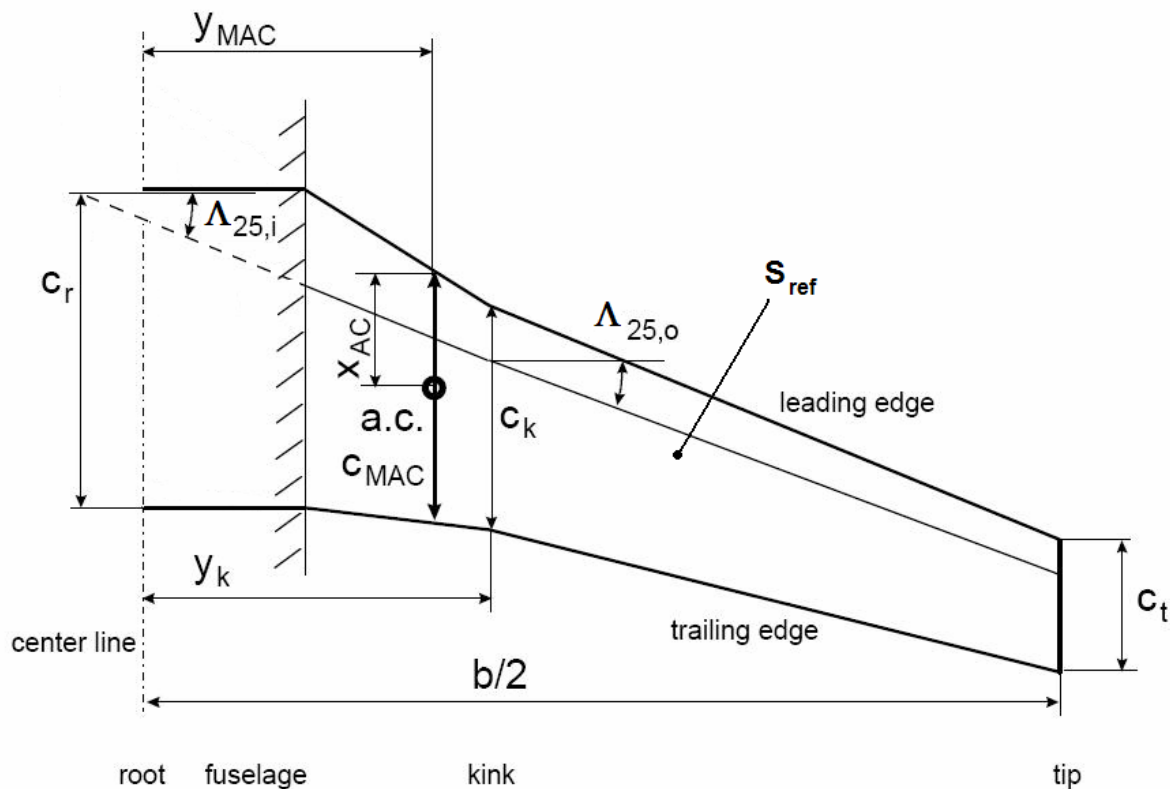


**Figure 1.1** Wing top view and geometry definitions (based on Scholz 1999)

The choice of this wing area is arbitrary, since later in the design process, when actual wing area values are required one can multiply all calculated values by the  $S_{eff}/S_{ref}$  ratio. This wing

area differs also from aircraft manufacturer to manufacturer (or even per project). In Figure 1.2 the definitions according to *Boeing*, *Airbus*, *Fokker* and *MD* can be seen. Later in this work and in the design tool we will use the Airbus definition of reference area.

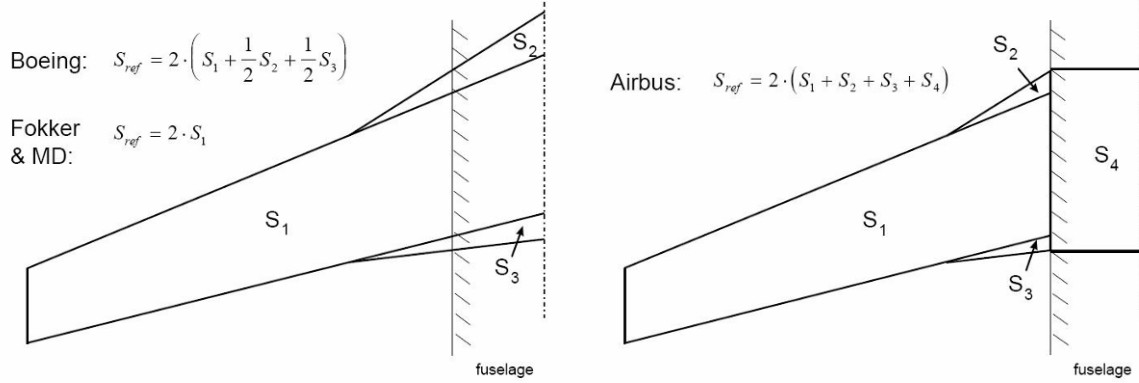


**Figure 1.2** Reference area  $S_{ref}$  definitions of Boeing and Airbus (**Scholz 1999**)

### Wing twist – aerodynamic and geometric

Aerodynamic twist can be defined as the difference between the zero lift angle of the tip airfoil and the zero lift angle of the root airfoil

$$\varepsilon_{t,a} = \alpha_{C_l=0,t} - \alpha_{C_l=0,r} \quad (1.1)$$

Geometric twist  $\varepsilon_t$  is defined as the difference between the angle of attack of the tip section and the root section of the wing.

$$\varepsilon_{t,g} = \alpha_t - \alpha_r \quad (1.2)$$

The total wing twist is the sum of the geometric and aerodynamic twist.

### Mean aerodynamic chord

The mean aerodynamic chord is defined as the chord on which the center of lift of the entire lifting surface is located. On a linear tapered, untwisted wing (trapezoidal wing) and with the assumption that lift is proportional to chord length the mean aerodynamic chord can be calculated as follows:

$$c_{MAC} = \frac{2}{3} \cdot c_r \cdot \frac{1 + \lambda + \lambda^2}{1 + \lambda} \quad (1.3)$$

The span of the mean aerodynamic chord for the same assumptions can be calculated as follows:

$$Y_{MAC} = \frac{b}{6} \cdot \left( \frac{1 + 2\lambda}{1 + \lambda} \right) \quad (1.4)$$



### Axes of an aircraft

In order to keep some consistence in the many dimensions concerning wing geometry that will be calculated, it is useful to define a coordinate system used for the entire aircraft. Figure 1.3 gives a clear representation of the different axes and also gives their name as used in stability definition.

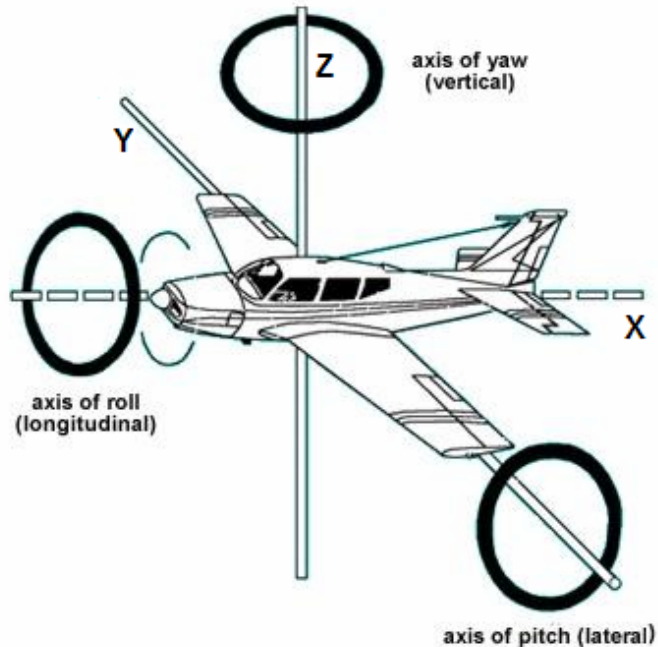


**Figure 1.3** Axes of an aircraft (based on [www.start-flying.com](http://www.start-flying.com))

### Spin (spin recovery)

A spin is a vertical movement of the aircraft combined with a rotating about a vertical axis, with the inside wing and the horizontal tail fully stalled. The aircraft is also at a large sideslip angle. (Raymer 2006, p.83)

### Critical Mach number $M_{cr}$

“The critical Mach number occurs when shocks first form on the aircraft.” (Raymer 2006, p.341) This shock waves increase the total drag, and the drag increase due to the shock waves is called Wave drag  $C_{D,w}$ . In Figure 1.4 the wave drag is shown as function of Mach number.

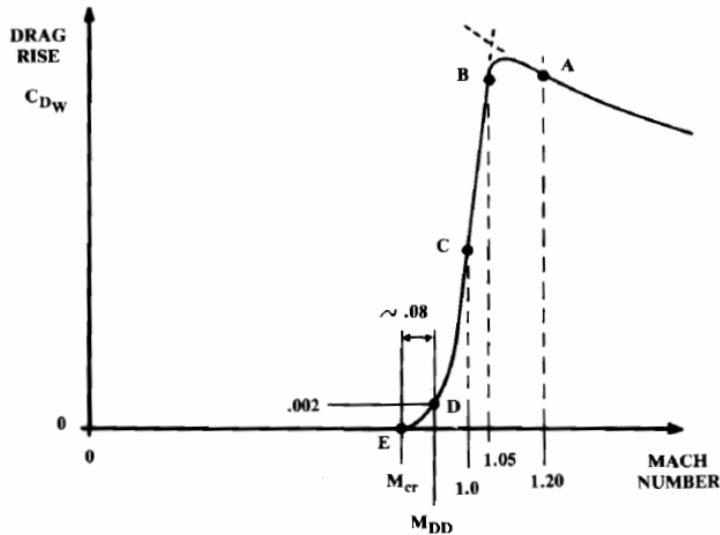


**Figure 1.4** Critical Mach number and Drag divergence Mach number (Raymer 2006, p.345)

### Drag divergence Mach number $M_{DD}$

“The drag divergence Mach number is the Mach number at which the formation of shocks begins to substantially affect the drag.” (Raymer 2006, p.341) The drag rise which determines the  $M_{DD}$  is arbitrary, and several definitions are in use. Airbus and Boeing use a wave drag rise of 20 drag counts or  $\Delta C_D = 0.0002$  according to (Raymer 2006, p.341). According to this definition, the  $M_{DD}$  is approximately 0.08 higher than  $M_{cr}$ , as can be seen in Figure 1.4.

## 1.5 Report structure

**Chapter 2** This chapter describes the conceptual design of the wing and high lift devices, starting from the design constraints and some input parameters from the early design phase. For every parameter which has to be selected by the user of the wing there are different guidelines based on different authors. It also describes the implementation in the tool.

**Chapter 3** This chapter describes the conceptual design of the empennage. This starts after the wing design. In this chapter it is not the goal to give an exact geometry calculated with the center of gravity, it only gives an initial estimation of the empennage geometry based on historical data. The implementation in the tool is also described.

**Appendix A** gives the source code of a macro to add airfoils to the library into excel.

## 2 Conceptual design of wings

There are various types of aircraft configurations each with its advantages and disadvantages, and each of them having a certain wing location. It is beyond the scope of the tool to include all the different configurations. The tool focuses on conventional configurations with high or low wing at high and low subsonic speeds. It therefore includes business jets, regional turbo-props and jet transport aircraft, as stated in the motivation.

The order of the paragraphs in this chapter is the same as the design process based on (**Roskam II 1985**, chapter 6). This is also the design order used in the excel worksheet:

1. Preliminary sizing input
2. Overall wing-fuselage arrangement
3. Sweep angle
4. Thickness ratio and thickness distribution
5. Airfoil selection
6. Lift distribution and chord distribution
7. Wing twist and incidence angle
8. Dihedral angle
9. Ailerons
10. High lift devices
11. Fuel tank estimation

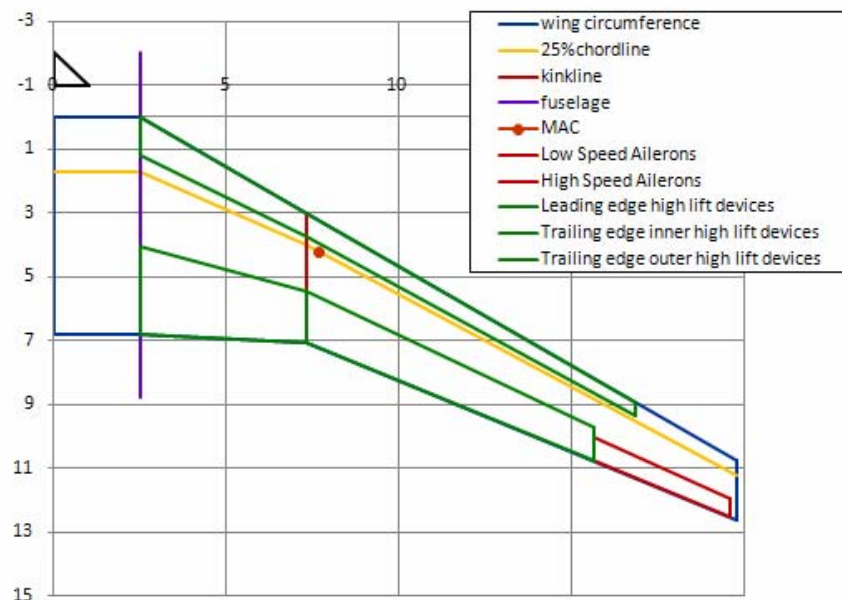


**Figure 2.1** Wing with all major parameters defined.

After all the parameters are selected the wing geometry is described as is given in Figure 2.1.

## 2.1 Design requirements

The wing of an aircraft has to fulfill certain aerodynamic requirements (e.g. high lift to drag ratio during cruise, enough lift capability during landing, enough climb capability to reach next flight level...). In addition there are also external requirements imposed by safety regulations, airport handling of the aircraft or even the market demand requirements (“if an aircraft does not sell, it will not be built”). Because all these requirements are already assigned, all of them together form a window in which each design constraint can be chosen and traded.

### 2.1.1 Cruise requirements

Obviously during cruise the wing has to produce enough lift to carry the aircraft and its payload over a certain distance, but there are also other requirements during cruise which need to be fulfilled, which can be seen in Figure 2.2.

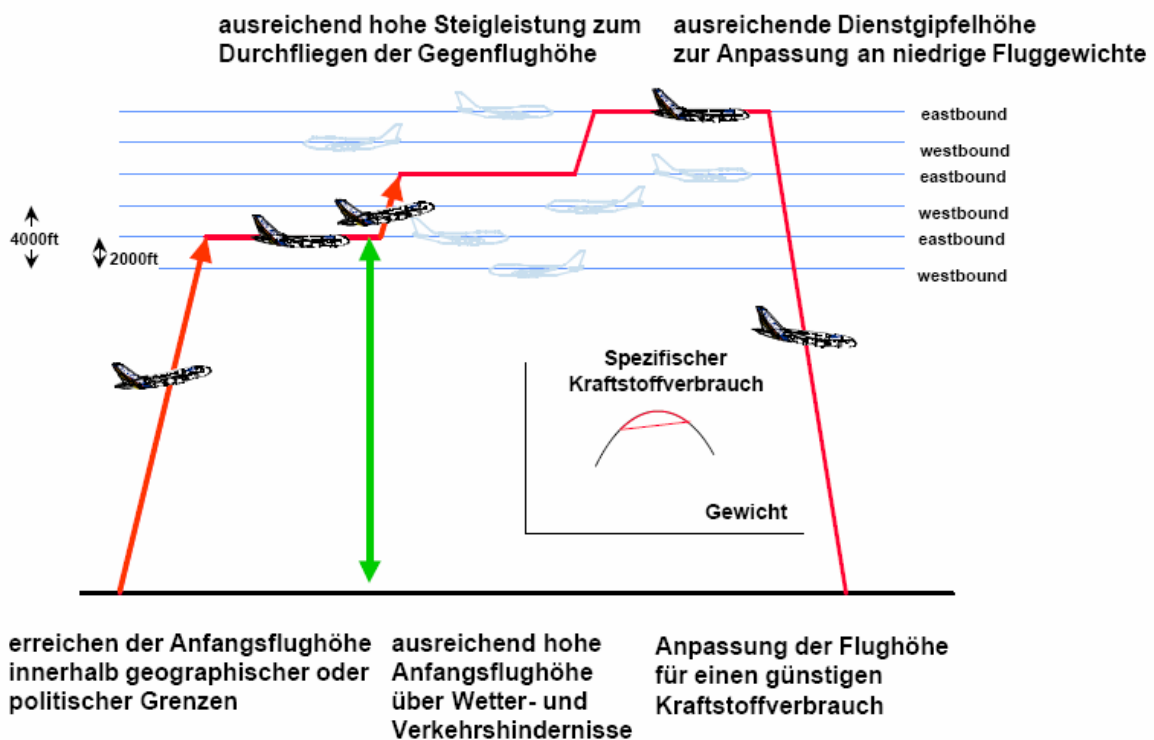


**Figure 2.2** Typical climb schedule (Böttger 2004)

The aircraft needs to maintain enough climb capability to reach him the next flight level or to avoid bad weather conditions and obstacles. The aircraft also needs enough climb capability to reach cruise level within an acceptable time (~20min) and range (200nm for long range). (Böttger 2004)

## 2.1.2 Take off and landing requirements

An airport field length is limited and therefore it is necessary that the aircraft can take off and land within those imposed limits. Nowadays, with ever growing noise reduction measures, the climb and descent ratios of aircraft can become even more stringent.

A short field length can be obtained using a higher wing area, more take-off thrust or increasing the take-off lift coefficient  $C_{L,TO}$ . The latter depends on the used high lift devices (see section 2.10) and the tail shape, which determines the maximum angle of attack during take-off.

A short landing field length can be obtained with a low approach speed and an efficient braking system after touchdown. (Landing gear, spoilers, thrust reversers...) The approach speed is determined by a trade-off between landing lift coefficient  $CL,L$  and Wing area  $S$ .

## 2.1.3 Taxi and terminal requirements

In the airport, all aircraft have to be operated using the existing terminal infrastructure. This can put limits to various design constraints. For example the wingspan can be limited to a certain value for a give aircraft type. Typical values of wing span limits can be seen in Table 2.1.

**Table 2.1** Typical airliner wing span limits (Howe 2000, p126)

Aircraft range	Typical wingspan [m]
Commuter/regional Narrow body	20 – 21.5
Short Range	28.5
Long Range	34
Wide body	
Med./Long Range	50
Long Range	61
Ultra high capacity	77-80

## 2.1.4 Operation

In order to be able to certify an aircraft, all certification requirements for a safe operation of the aircraft have to be fulfilled. In case of an emergency, inflatable slides at the passenger doors are used to evacuate all the passengers within the given time limit (usually 90 seconds). These slides have to maintain a minimum distance from the wing structure and the power plants. This can put a limit to root chord of the wing.

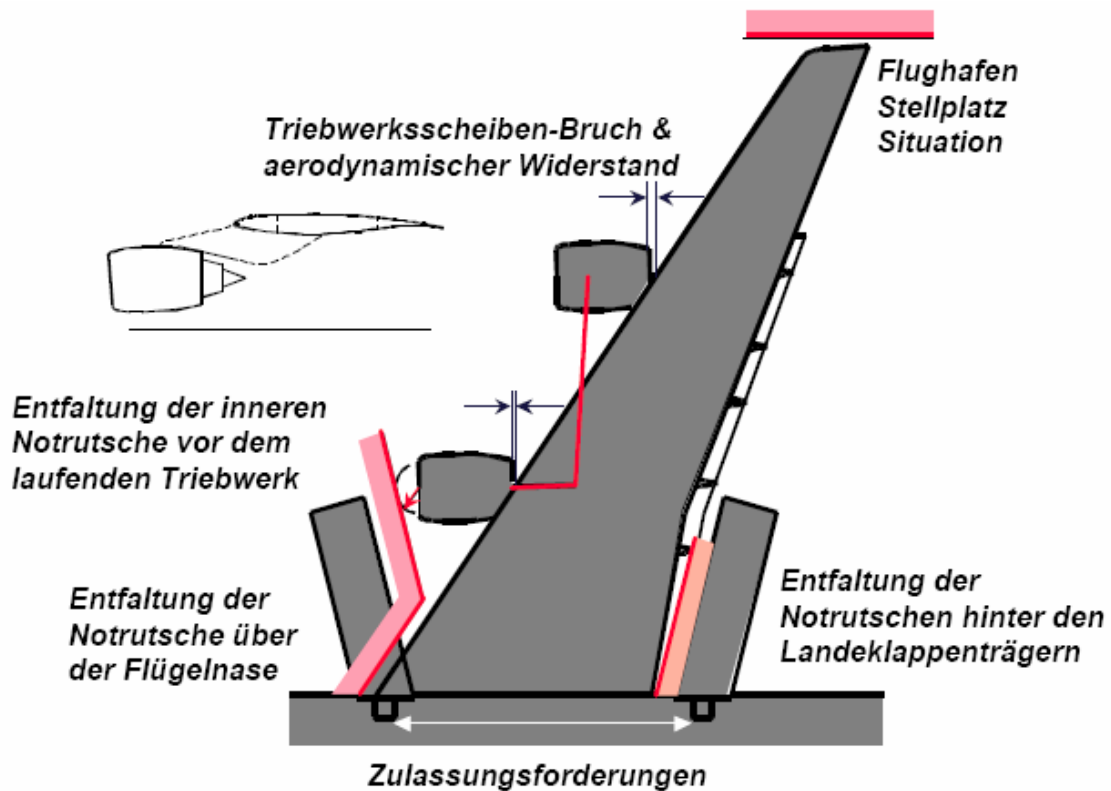


Figure 2.3 Design requirements of a wing (Böttger 2004)

## 2.2 Input parameters from earlier design phases

During wing design some earlier designated wing parameters have to be taken into account. Below a brief discussion is given about the needed input design parameters. In the tool these values have to be inserted as input values, as can be seen on Figure 2.4.

1 preliminary sizing data			
max take off weight	$m_{MTO}$	<input type="text" value="100 000"/> [kg]	Wing loading $W/S$ <input type="text" value="625.00"/> [kg/m <sup>2</sup> ]
wing area	$S_{ref}$	<input type="text" value="160.00"/> [m <sup>2</sup> ]	
Fuselage diameter	$d_f$	<input type="text" value="5.00"/> [m]	
cruise mach number	$M_c$	<input type="text" value="0.85"/> [-]	
cruise lift coefficient	$C_{Lc}$	<input type="text" value="0.5"/> [-]	
<input checked="" type="radio"/> Aspect ratio	$AR$	<input type="text" value="9.81"/> [-]	→ Wing Span $b$ <input type="text" value="39.62"/> [m]
<input type="radio"/> Wing Span	$b$	<input type="text" value="38.00"/> [m]	→ Aspect ratio $AR$ <input type="text" value="9.03"/> [-]

The graph shows lift coefficient (y-axis, -3 to 15) versus Mach number (x-axis, 0 to 20). It features several curves representing different wing configurations, with a vertical line at Mach 0.85 and a horizontal line at CLc = 0.5.

2 Overall wing - fuselage arrangement	
select wing - fuselage arrangement	<input type="text" value="low wing"/>

The graph shows the wing geometry and fuselage arrangement, with the x-axis representing spanwise distance (0 to 20) and the y-axis representing vertical distance (-3 to 3). It includes a curved line for the wing profile and a horizontal line for the fuselage.

Figure 2.4 Preliminary sizing input data as implemented in the tool.

### 2.2.1 Maximum take off mass and wing loading

The maximum take off weight or  $m_{MTO}$  determines together with the wing loading the required wing area  $S$  or  $S_{ref}$ . So the  $m_{MTO}$  and the wing loading determine the size of the wing. In the tool it is actually the reference area that is required and the wing loading is then calculated.

### 2.2.2 Fuselage diameter

Since the area inside the fuselage contributes to the wing reference area, it has an influence on the actual wing geometry and is therefore required as input parameter in the wing design phase.

### 2.2.3 Aspect ratio

In a first approach we use the value of the aspect ratio which was already assigned during the preliminary sizing. If however during the wing design some early defined design requirement (e.g. airport handling maximizing span, emergency exit installation maximizing root chord... see paragraph 2.1) cannot be fulfilled using the given aspect ratio, it can still be changed according to the requirement. But keep in mind that this changes the preliminary sizing process and thus the sizing will have to be redone.

### 2.2.4 Cruise Mach number $M_c$

This number is very decisive for the aerodynamic characteristics of the airflow over the wing and has therefore a high influence on the actual wing geometry. The cruise Mach number is one of the major design constraints. Many of the first estimations are based upon the cruise Mach number.

### 2.2.5 Cruise lift coefficient $C_{L,C}$

The cruise lift coefficient is known after the preliminary sizing process because the  $m_{MTO}$ , the  $m_{ML}$ , the wing loading and the cruise height are known; by using the lift equation we now find the cruise lift coefficient.

## 2.2.6 General wing-fuselage arrangement

As general wing-fuselage arrangement we have three options: high wing, low wing and mid wing. In practice only the first two are used, the latter is only usable on small aircraft, up to a few passengers. In a mid-wing configuration, the wing box needed for the wing installation would split a long fuselage cabin into two different compartments, which has an obvious disadvantage for both passenger and cargo transport aircraft.

Both high and low wing have their own advantages, which are discussed in (Scholz 1999, Table 7.1). In brief we can say that a high wing is good for engine integration under the wings, short landing gear and a low-to-the-ground cargo floor. The low wing however has advantages concerning landing gear integration and a lighter fuselage section in the center of the wing.

As a general rule, a high wing is only selected if needed for engine integration or if the payload/cargo floor should be close to the ground; in all other cases, the low-wing is preferred.

## 2.3 Thickness to chord ratio and sweep angle

### 2.3.1 Low subsonic

The border between low and high subsonic speed can be described as the cruise Mach number at which it becomes advantageous to use a swept wing. It is very difficult to give an exact value of Mach number which describes this border, because it depends on Cruise lift coefficient and technology standard of the airfoil used. On Figure 2.6 the border is located somewhere around Mach 0.6 according to (Raymer 2006, Figure 4.20).

According to (Howe 2000, p118) it can be derived from equation 2.6 that the zero sweep angle should be located at the Mach number given by this equation.

$$M_{DD} = 0.95 - 0.1 \cdot C_{L,C} - t/c \quad (2.1)$$

At low cruise Mach numbers the thickness of the used airfoil is determined by airfoil aerodynamics; thus an airfoil with good lift to drag characteristics in the cruise condition of the aircraft. The selected airfoil gives then a range of airspeeds where the optimized lift to drag characteristics are valid.

A first estimation can be made based on (Raymer 2006, Figure 4.20) and is based on cruise Mach number. On Figure 3.2 we can see the guideline in Figure 2.6 as the blue line. The equation of the linear regression of this line is:



$$t/c = -0.02099 \cdot M_c + 0.15594 \quad (2.2)$$

Another guideline could be the non-linear regression; this is a regression of statistical aircraft data over various parameters of influence on thickness to chord. The regression is given by equation 2.7 (Ciornei 2005). In this equation at low subsonic speeds we have to assume an unswept wing and normally the airfoil technology factor  $k_m$  should be the one of a conventional airfoil (e.g. NACA 6 or 5 series). To see the effect of the  $k_m$  factor on thickness, different values for  $k_m$ , which can be seen in Table 2.2, are selected in the graph below (see Figure 2.5)

Below Mach numbers of 0.2 the non-linear regression guideline loses its meaning because Mach number has a negative power in the equation so at Mach number 0 the suggestion goes to infinity

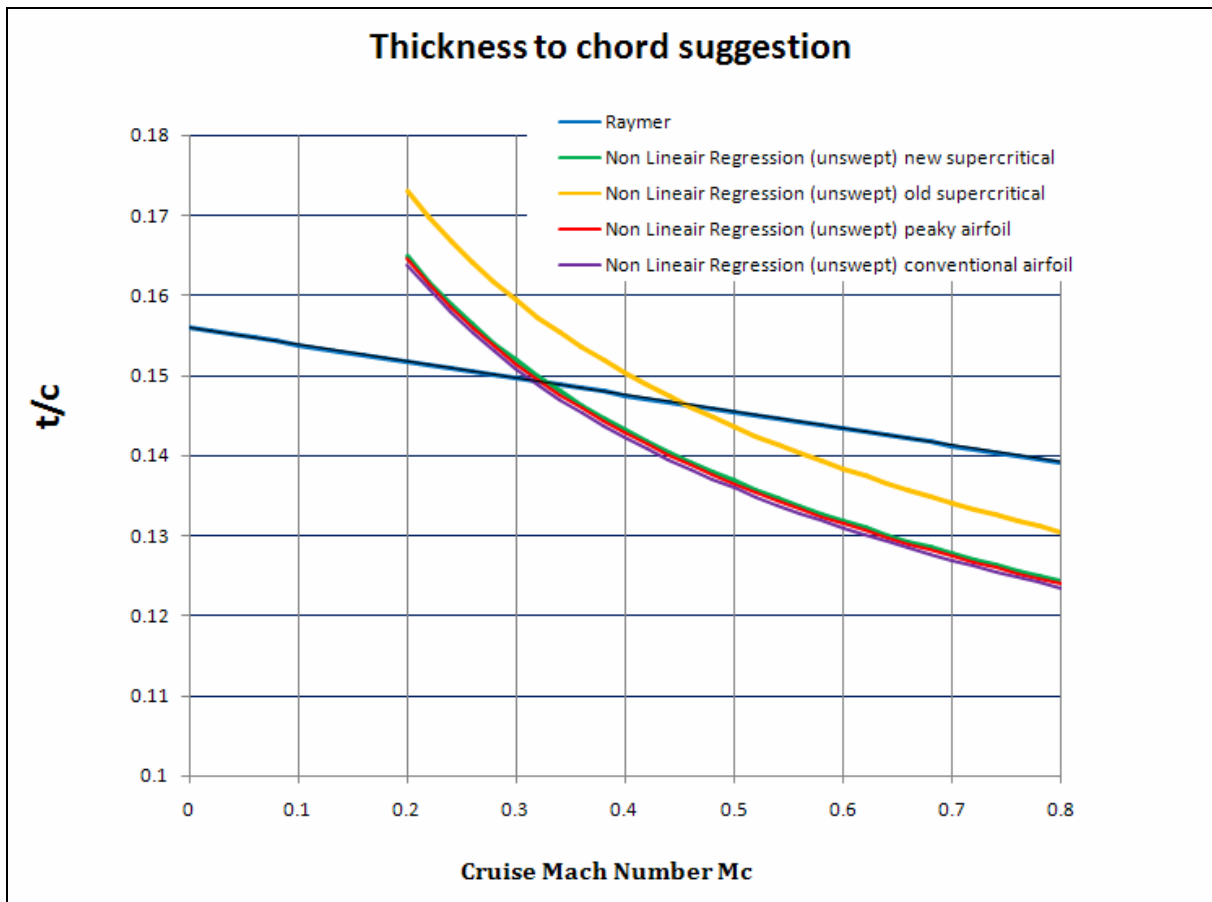


**Figure 2.5** Thickness to chord suggestions for low subsonic Mach numbers

The different thickness to chord suggestions are presented in the graph seen in Figure 2.5. If we now place a design point on this graph, the comparison between different guidelines and the selected design can be seen clearly.

### 2.3.2 High subsonic

At high subsonic cruise Mach numbers (above the border discussed in paragraph 2.3.1) there is a need for wing sweep in order to increase the absolute thickness of the wing without excessive drag rise due to shock waves. An elaborate explanation can be found in (Torenbeek 1988, paragraph 7.5.1).

A first estimation, based on cruise Mach number, can be made using the guideline for leading edge sweep according to (Raymer 2006, Figure 4.20) given in Figure 2.6. In the tool this graph is converted to quarter chord sweep in order to make it more convenient for the user to compare it with other guidelines.

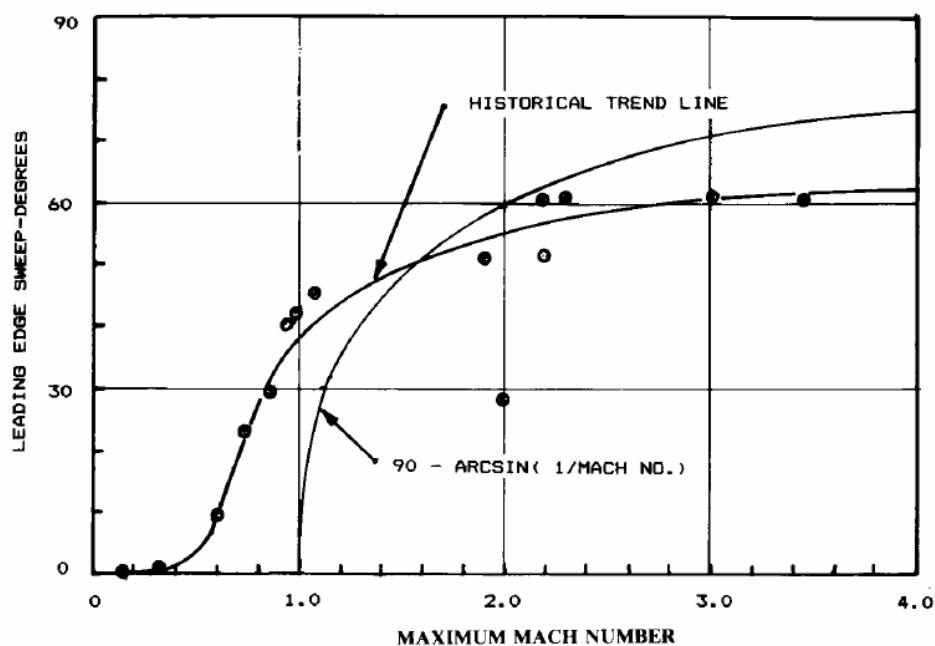


**Figure 2.6** Leading edge sweep suggestion (Raymer 2006, Figure 4.20)

With the sweep angle chosen there are a few equations which give an estimation of the average thickness to chord ratio. (Howe 2000) and (Torenbeek 1988) give an approximation based on semi-empirical equations, and give the maximum allowable thickness to chord ratio in function of a given sweep angle and cruise Mach number. It is therefore wise not to exceed these limits.

The non linear regression gives an approximation based on statistical data and gives therefore differs from the two latter in that way that it doesn't represent the trade of between sweep and thickness. It rather represents the most commonly used thickness at a given sweep angle.



**Figure 2.7** Different guidelines of thickness to chord suggestions.

The different suggestions are summarized in a graph which gives the thickness to chord in function of quarter chord sweep angle, as seen in Figure 2.7. To make it more convenient for the user, the design point is also represented in the graph by a red dot.

All three equations used as thickness guidelines are explained below.

- **Torenbeek**

According to **(Torenbeek 1988)** the relation between wing thickness ratio, sweep angle, drag divergence Mach number and cruise lift coefficient is given by the following equation.

$$t/c = 0.3 \cos \Lambda_{25} \left( \left[ 1 - \left( \frac{5 + M_{DD,eff}^2}{5 + (k_M - 0.25 \cdot C_L)^2} \right)^{3.5} \right] \cdot \frac{\sqrt{1 - M_{DD,eff}^2}}{M_{DD,eff}^2} \right)^{\frac{2}{3}} \quad (2.3)$$

The factor  $k_m$  takes the technology standard of the airfoil into account and can be read in Table 2.2 for various airfoil types. This theoretical equation is actually only valid in regions of undisturbed 2D flow, where the effective drag divergence Mach number is the component of the free stream drag divergence Mach number perpendicular to the leading edge, as can be seen in Figure 2.8.

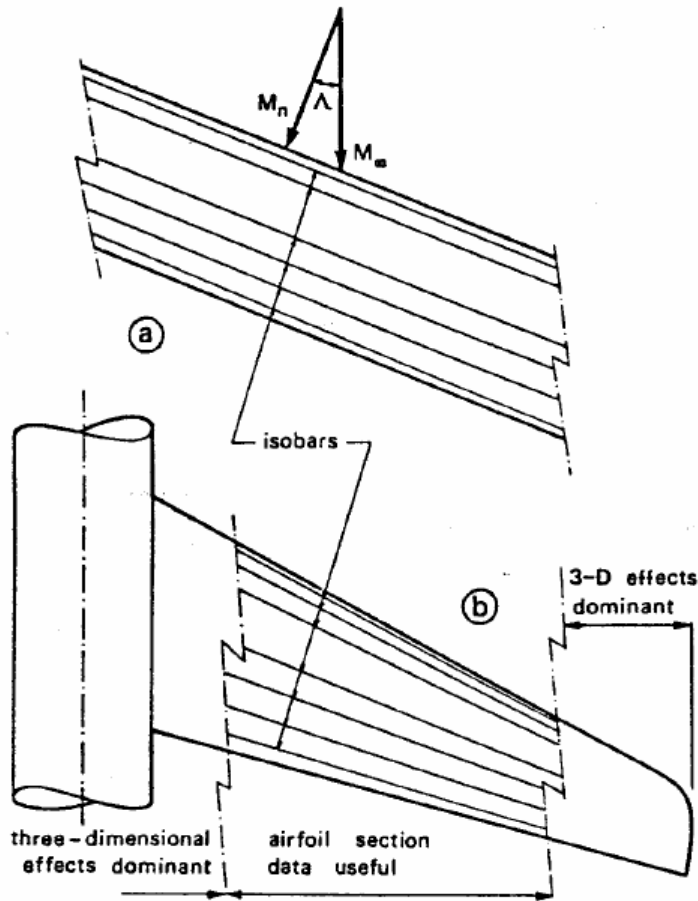


**Figure 2.8** 2-D and 3-D flow characteristics over the wing (Torenbeek 1988)

As the wing is not infinite, at the wingtip and root 3-D flow effects take place. Therefore the effective drag divergence Mach number is given by the following equation. (Torenbeek 1988)

$$M_{DD,eff} = M_{DD} \cdot \sqrt{\cos \Lambda_{25}} \quad (2.4)$$

- **Howe**

According to (Howe 2000, p118) the thickness to chord can be given by following equation

$$t/c = 0.95 - 0.1 \cdot C_{L,C} - M_{DD,eff} \quad (2.5)$$

In combination with equation 2.4 for effective drag divergence number this gives as

$$t/c = 0.95 - C_{L,C} - M_{DD} \cdot \sqrt{\cos(\Lambda_{25})} \quad (2.6)$$

- **Non-linear regression**

Another guideline based on a non-linear regression of statistical aircraft data over various parameters of influence on thickness to chord. The regression is given by the following equation according to (Ciornei 2005).

$$t/c = 0.127 \cdot M_{DD}^{-0.204} \cdot (\cos(\Lambda_{25}))^{0.573} \cdot C_{L,C}^{0.065} \cdot k_m^{0.556} \quad (2.7)$$

The parameter  $k_m$  depends on airfoil technology standard and can be read in

**Table 2.2**  $k_m$  Factors in thickness equations (Ciornei 2005 & Scholz 1999)

Airfoil type	Non linear regression	Torenbeek
conventional	0.921	1.00
high speed (peaky)	0.928	1.05
old supercritical	1.017	1.10
new supercritical	0.932	1.20

### 2.3.3 Thickness distribution

The variable thickness along the wing span is the thickness distribution of the wing. The actual thickness at a certain location is very depending on 3-D flow characteristics. Exact calculations require advanced aerodynamic software. It is therefore that an initial thickness distribution, according to (Jenkinson 1999) is used. This is an initial distribution, but gives a good approximation of the real wing.

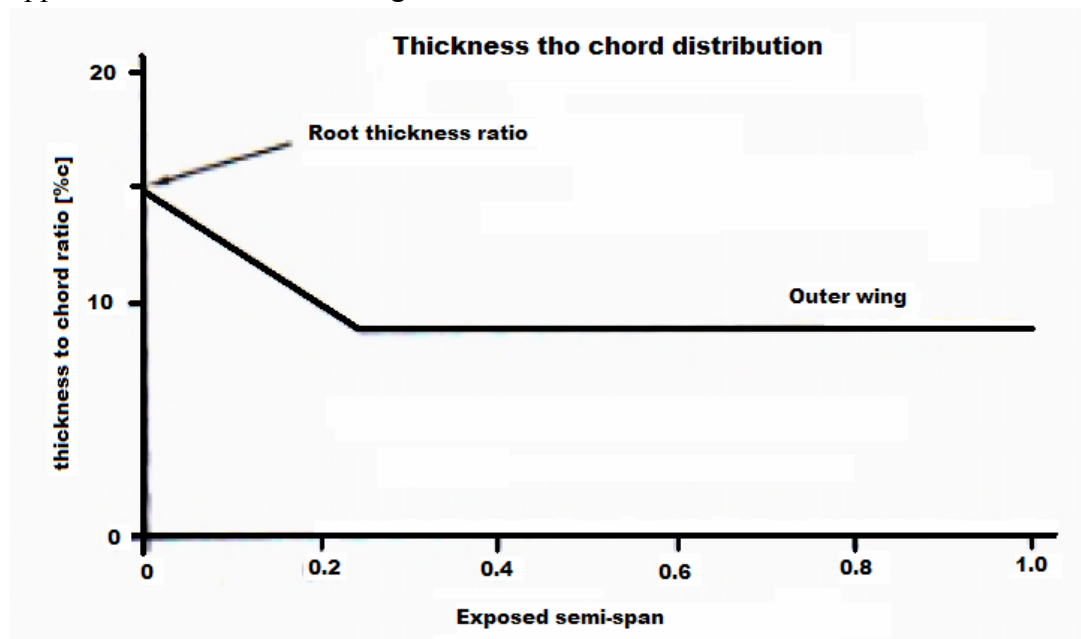


**Figure 2.9** Thickness to chord distribution. (based on Jenkinson 1999)

According to (**Jenkinson 1999**) the average thickness ratio or  $(t/c)$  can be found as follows.

$$(t/c) = \frac{3 \cdot (t/c)_t + (t/c)_r}{4} \quad (2.8)$$

Since equation (2.3), 2.6 and 2.7 give an initial value for the average thickness ratio, the thickness at the wing root and tip can be found using equation 2.8. This gives following equations for root and tip thickness ratio.

$$(t/c)_r = \frac{4}{(3 \cdot \tau + 1)} \cdot (t/c) \quad (2.9)$$

$$(t/c)_r = \frac{\tau \cdot 4}{(3 \cdot \tau + 1)} \cdot (t/c) \quad (2.10)$$

With

$$\tau = \frac{(t/c)_t}{(t/c)_r} \quad (2.11)$$

According to (**Howe 2000**, Table 5.3) the tip chord should be approximately 65% of the root chord for both low and high subsonic. Thus a good initial value for  $\tau$  is 0.65.

### 2.3.4 Sweep angle geometry calculations

Since the wing is usually double tapered, the inner and outer trapezoid have different sweep angles. In order to calculate the different sweep angles, the aspect ratios of inner and outer wing have to be known. These can be found using following equations.

$$A_i = \frac{(Y_k - f_d / 2)}{S_i} \quad (2.12)$$

$$A_o = \frac{(b/2 - Y_k)}{S_o} \quad (2.13)$$

In paragraph 2.3.2 the term wing quarter chord sweep angle is used, although there is actually no general wing quarter chord sweep angle. As an approximation the outer trapezoid quarter chord sweep angle will be used as the wing quarter chord sweep angle. This can be done because the outer wing is the largest part of the wing and the inner part of the wing usually has almost the same quarter chord sweep angle as there is usually only one leading edge sweep angle.

$$\Lambda_{25} = \Lambda_{25o} \quad (2.14)$$

With the quarter chord sweep angle of the inner and outer wing known, it is possible to calculate the sweep angle at any constant percent chord line using following equation, where  $\Lambda_{x,y}$  is the sweep angle at constant x percent chord line in the y trapezoid part of the wing.

$$\Lambda_{x,y} = \text{Arc tan} \left[ \tan(\Lambda_{25,y}) - \frac{4}{A_y} \cdot \frac{(x-25)}{100} \cdot \frac{(1-\lambda_y)}{(1+\lambda_y)} \right] \quad (2.15)$$

With  $\lambda_y$  is the taper ratio of the specific trapezoid and  $A_y$  the aspect ratio of the specific trapezoid. This equation is used to obtain the  $\Lambda_{LE}$ , the  $\Lambda_{TE}$  and the  $\Lambda_{50}$  for both the inner and outer wing.

Since the wing usually has only one leading edge and the quarter chord sweep angle of the inner trapezoid is required, a suggestion for  $\Lambda_{25i}$  is given which leads to an equal leading edge sweep of inner and outer trapezoid. The suggestion is given by following equation.

$$\Lambda_{25i} = \text{Arc tan} \left[ \tan(\Lambda_{25,o}) + \frac{(1-\lambda_o)}{A_o \cdot (1+\lambda_o)} \right] - \frac{(1-\lambda_i)}{A_i \cdot (1+\lambda_i)} \quad (2.16)$$

The implementation in the tool is based on the inner and outer quarter chord sweep angle selection and the thickness to chord can be selected, according to the different authors. The airfoil technology standard is also required for the suggestions according to (Torenbeek 1988) and (Ciornei 2005). The definition of mach drag divergence number (see paragraph 1.4) can also be selected according to own standards. The implementation can be seen in Figure 2.10. The relative thickness ratio  $\tau$  can be given for the inner and outer wing, but the values given are actually sufficient accurate for the conceptual design.

3 Sweep							
outer Sweep angle	$\Lambda_{26,o}$	<input type="text" value="30.00"/>	[ ° ]	sweep LE	$\Lambda_{LE,o}$	<input type="text" value="31.89"/>	[ ° ]
↑	howe	<input type="text" value="30.53"/>	[ ° ]	sweep 50%c	$\Lambda_{50,o}$	<input type="text" value="28.04"/>	[ ° ]
↑	raymer	<input type="text" value="27.55"/>	[ ° ]	sweep TE	$\Lambda_{TE,o}$	<input type="text" value="23.88"/>	[ ° ]
				Sweep x%c	x=	<input type="text" value="25"/>	<input type="text" value="30.00"/>
							[ ° ]
inner Sweep angle	$\Lambda_{26,i}$	<input type="text" value="25.72"/>	[ ° ]	sweep LE	$\Lambda_{LE,i}$	<input type="text" value="31.89"/>	[ ° ]
↑	single leading edge	<input type="text" value="25.72"/>	[ ° ]	sweep 50%c	$\Lambda_{50,i}$	<input type="text" value="18.84"/>	[ ° ]
				sweep TE	$\Lambda_{TE,i}$	<input type="text" value="3.45"/>	[ ° ]
				sweep x%c	x=	<input type="text" value="25"/>	<input type="text" value="25.72"/>
							[ ° ]
4 thickness ratio and thickness distribution							
Select airfoil technology	<input type="text" value="new supercritical"/>						
mach drag divergenc definitior	$\Delta_{MDD}$	<input type="text" value="0"/>		drag diverg mach n°	$M_{DD}$	<input type="text" value="0.850"/>	[ - ]
thicknes to chord ratio	t/c	<input type="text" value="0.1111"/>	[ - ]		$M_{DDeff}$	<input type="text" value="0.791"/>	[ - ]
↑	raymer	<input type="text" value="0.1381"/>	[ - ]				
↑	torenbeek	<input type="text" value="0.0947"/>	[ - ]	root thickness ratio	(t/c)r	<input type="text" value="0.151"/>	[ - ]
	km	<input type="text" value="1.15"/>	[ - ]	tip thickness ratio	(t/c)t	<input type="text" value="0.098"/>	[ - ]
↑	non linear regression	<input type="text" value="0.1111"/>	[ - ]	kink thickness ratio	(t/c)k	<input type="text" value="0.098"/>	[ - ]
	km	<input type="text" value="0.932"/>	[ - ]				
Inner relative thickness rati	$\tau_i$	<input type="text" value="0.65"/>	[ - ]	relative thickness ratio	$\tau$	<input type="text" value="0.650"/>	[ - ]
Outer relative thickness rati	$\tau_o$	<input type="text" value="1"/>	[ - ]				

Figure 2.10 Sweep angle and thickness selection as implemented in the tool.

## 2.4 Airfoil section

The main lift producing form on the aircraft is the airfoil section of the wing. The shape is highly dependent upon general configuration, cruise Mach number and mission of the aircraft. Detailed airfoil design is done using aerodynamic software and wind tunnel tests, but for the early design it is sufficient to work with “simple” airfoils which have known lift, drag and pitching moment characteristics.

A family of such airfoils is the NACA airfoil series; although these airfoils are quite old they form a good basis to start the airfoil selection from, because the geometry can quite easily be calculated and lift and drag characteristics are widely spread in specified literature. (**Abbott and Von Doenhoff 1959**)





- NACA 23015** 0 stands for non reflexed trailing edge and 1 stands for a reflexed trailing edge. [DATCOM 1978]
- NACA 23015** The maximum thickness in percent of the chord  
Maximum thickness =  $0.15c$

An example can be seen in Figure 2.12.

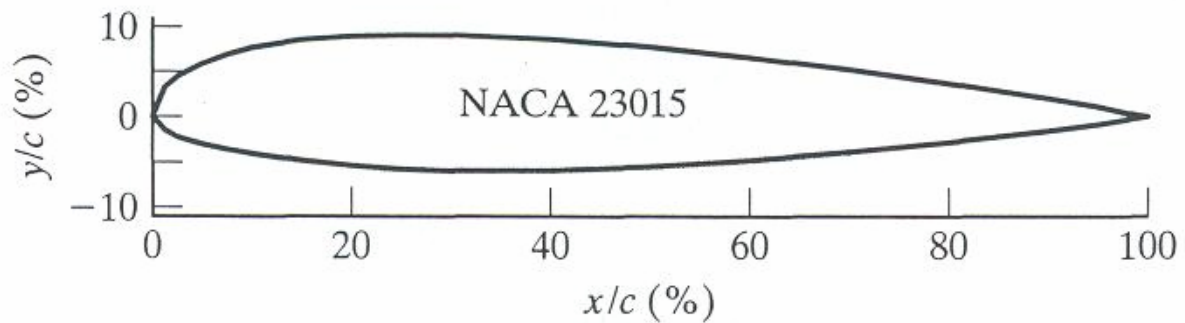


**Figure 2.12** NACA 23015 airfoil (Corke 2003)

- **4 and 5 modified series**

The NACA four and five digit series have a fixed position of the maximum thickness and a certain leading edge radius. The modified series were developed to make it possible to modify the values of these parameters. They consist of the four/five digit number followed by a dash (“-”) and two digits. The first of the two indicates the nose radius index and the second is the location of maximum thickness in tenths of chord aft of the leading edge.

The nose radius index is an arbitrary number assigned to the leading edge, a value of 0 describes a sharp nose while a value of 6 yields the same nose radius as the normal four digit series. When the index is 9, the nose radius is 3 times higher than with the normal four digit series.

For example NACA 2412-45 has its maximum camber at  $0.4c$  and a nose radius which is slightly smaller than a regular NACA 2412 airfoil.

- **6 series**

The NACA 6 series airfoils are designed to maximize laminar flow; which gives them good base drag characteristics.

**NACA 65<sub>2</sub>-415** Series designation

**NACA 65<sub>2</sub>-415** Point of minimum pressure in tenths of chord.  
Minimum pressure  $0.5c$

**NACA 65<sub>2</sub>-415** Describes the range of lift coefficient in tenths above and below the design lift coefficient in which favorable pressure gradients exist on both surfaces. (And thus where the drag maintains low)

Drag coefficient minimal over a range of lift coefficients of 0.2 above or below the design lift coefficient.

**NACA 65<sub>2</sub>-415** The design lift coefficient in tenths

Design lift coefficient 0.4

**NACA 65<sub>2</sub>-415** The maximum thickness in percent of the chord

Thickness to chord 0.15c

The extension “a=” followed by a number indicates the length of the laminar flow starting from the leading edge in units chord length. An example can be seen in Figure 2.13.

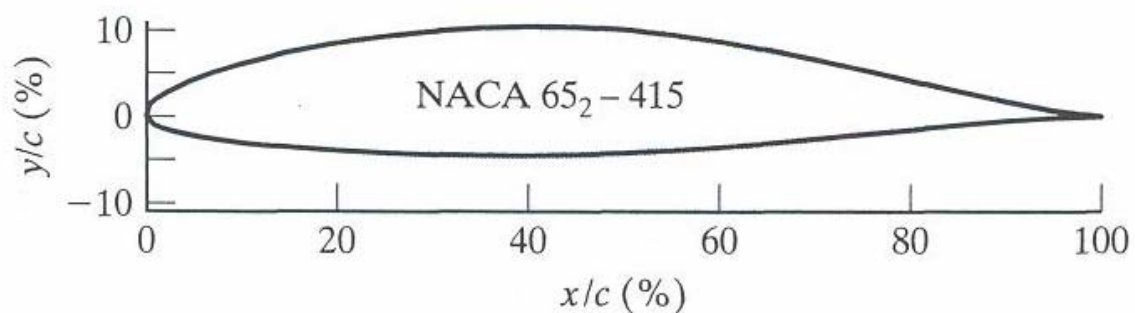


**Figure 2.13** NACA 65<sub>2</sub>-415 airfoil (Corke 2003)

- 7 series

The NACA 7 series airfoils was created to further advance the maximization of laminar flow over the profile. This was achieved by separately identifying the low pressure zones on upper and lower wing surfaces; and thus maximizing the laminar flow on upper and lower surface independently.

**NACA 747A315** Series designation

**NACA 747A315** Location of minimum pressure on the upper surface in tenths of chord length.

Upper surface position of minimum pressure 0.4c

**NACA 747A315** Location of minimum pressure on the lower wing surface in tenths of chord length.

Upper surface position of minimum pressure 0.7c

**NACA 747A315** The thickness distribution and the mean line forms used. This letter refers to a standard profile from earlier NACA series.

**NACA 747A315** Design lift coefficient in tenths

Design lift coefficient 0.3

**NACA 747A315** Maximum thickness in percent of chord length.

Maximum thickness 0.15c

The extension “a=” followed by a number indicates the length of the laminar flow starting from the leading edge in units chord length.

- 8 series

The NACA 8 series was designed for flight at supercritical speeds. Like the earlier airfoils, the goal was to maximize the extent of laminar flow on the upper and lower surface independently.

The numbering is identical to the 7 series, with the difference that the first digit is an “8” indicating the 8 series.

### 2.4.2 Airfoil selection

In the tool the user can select airfoils out of an airfoil data spread sheet, this is a sheet containing different airfoil coordinates. This sheet can be created using a macro in a second excel worksheet which contains macros to input airfoil coordinate files.

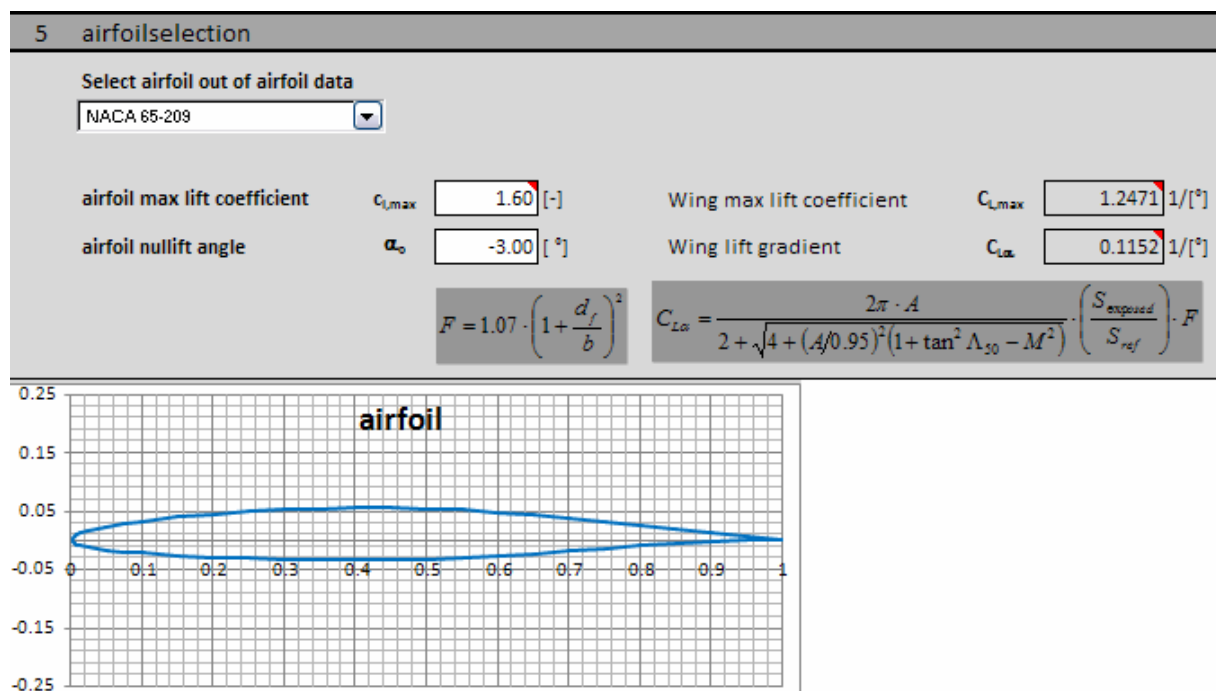
used by macro for input of airfoil files	counting number of airfoils	list of airfoil names to generate selection list	description of first airfoil		N	O	P	Q	R	S
A	B	C	D	E	F	G	H	I	J	K
1										1 NACA 747A415
2										1 NACA 747A315
3										1 NACA 67,1-215
4										1 NACA 66(4)-221
5										1 NACA 66(3)-418
6										1 NACA 66(3)-218
7										1 NACA 66(2)-415
8										1 NACA 66(2)-215
9										1 NACA 66-210
10										1 NACA 66-209
11										1 NACA 66-206
12										1 NACA 66(1)-212
13										1 NACA 66-018
14										1 NACA 65(4)-421 a=0.5
15										1 NACA 65(4)-421
16										1 NACA 65(4)-221
17										1 NACA 65-410
18										1 NACA 65(3)-218
19										1 NACA 65(2)-415 a=0.5
20										1 NACA 65(2)-415
21										1 NACA 65(2)-215
22										1 NACA 65-210
23										1 NACA 65-209
24										1 NACA 65-206
25										1 NACA 65(1)-412
26										1 NACA 65(1)-212 a=0.6
27										1 NACA 65(1)-212

Figure 2.14 Screenshot of airfoil data spread sheet.

The spread sheet used to store the airfoil coordinates is called “airfoil data”, as can be seen in Figure 2.14. The first nine columns are used by the macro for the input of airfoil files and should stay empty. The J-column is used to count the number of airfoils and the K-column stores the list of airfoil names from which can be selected and the rest of the columns is used for airfoil data. For reasons of simplicity each airfoil uses two columns, so that is possible for the user to manually add airfoils if needed. If done so, the name of the airfoil has to be added in the K-column at the exact vertical position.

These airfoil coordinate files are standard text files which have to have the first line being the name of the airfoil and from the second line up to maximum thousand lines with each a defining a point of the airfoil. The first number being the position on the chord (as a ratio with respect to the chord length) and the second being the height of the specific point above (or under) the chord line.

In general such a file starts with the point of the trailing edge, then describes the points of the upper surface from trailing edge to leading edge, and then describes the points of the lower surface from leading edge to trailing edge. One airfoil can be described using a maximum of thousand points in the tool. The source code of the macro used to input airfoil data can be found in appendix A.



**Figure 2.15** Airfoil selection as implemented in the tool.

The selection of the airfoil can be done in the *wing design* worksheet and can be seen in Figure 2.15. The airfoil zero lift angle and maximum lift are also required as input parameters. the calculation of the maximum lift coefficient of the wing and lift gradient is explained in paragraph 2.10.

### 2.4.3 Airfoil properties

If an airfoil is selected, some lift characteristics still have to be given. The zero lift angle of attack or  $\alpha_{c_l=0}$  is needed to calculate the incidence angle.

The section maximum lift or  $c_{l,max}$  is needed to calculate the wing maximum lift. If this value is not given,  $c_{l,max}=1.6$  is a good first estimation according to (Howe 2000, Table 5.1).

## 2.5 Lift distribution

According to aerodynamics the minimal induced drag is achieved by creating an elliptical lift distribution over the wing. Experience has shown that this is not always the technical optimum, because an elliptical lift distribution generates a greater bending moment on the wing root than for example a triangular lift distribution. This requires a stronger wing root for an unchanging root thickness (thickness is limited by wave drag in high subsonic cruise speeds), and thus resulting in a heavier wing. Therefore in practice the lift distribution tend to be something between an elliptical and a triangular lift distribution, as can be seen on Figure 2.16.

Beste Aerodynamik:  
Elliptische Auftriebsverteilung



Besseres Gewicht:  
Nach innen verlagerte Auftriebsverteilung



**Figure 2.16** Difference between aerodynamic and weight optimal lift distribution (Böttger 2004)

To determine the lift distribution, there are three ways of manipulating the lift along the wing-span.

- Tapered wings: variable chord length along the span.
- Geometric twist: changing the angle of attack of the airfoil sections along the span.
- Aerodynamic twist: changing the shape of the airfoil along the span.

## 2.5.1 Wing twist

Aerodynamic twist is too complicated to take in to account during the conceptual design. It requires detailed studies of aerodynamic characteristics of different airfoil shapes and is highly dependent of 3-D flow characteristics over the wing. In conceptual design the aerodynamic twist is taken into account by using a few degrees of geometric twist, which can later partially be converted in aerodynamic twist.

Since we take no aerodynamic twist in to account in the conceptual design, the total wing twist is the same as the geometric twist, where we can make the assumption that the defined geometric wing twist also takes the later added aerodynamic twist into account.

The lift distribution on a twisted wing is slightly dependent on the angle of attack, so in order to avoid excessive changes in lift distribution, the wing twist should not be larger than  $-5^\circ$ . Typically a value of  $-3^\circ$  of wing twist is used during the conceptual design phase. (Raymer 2006, p.63)

## 2.5.2 Taper ratio

The lift distribution in a first approximation is dependent upon the product of local chord length and local section lift coefficient. The effect of taper ratio on lift distribution can be seen in Figure 2.17.

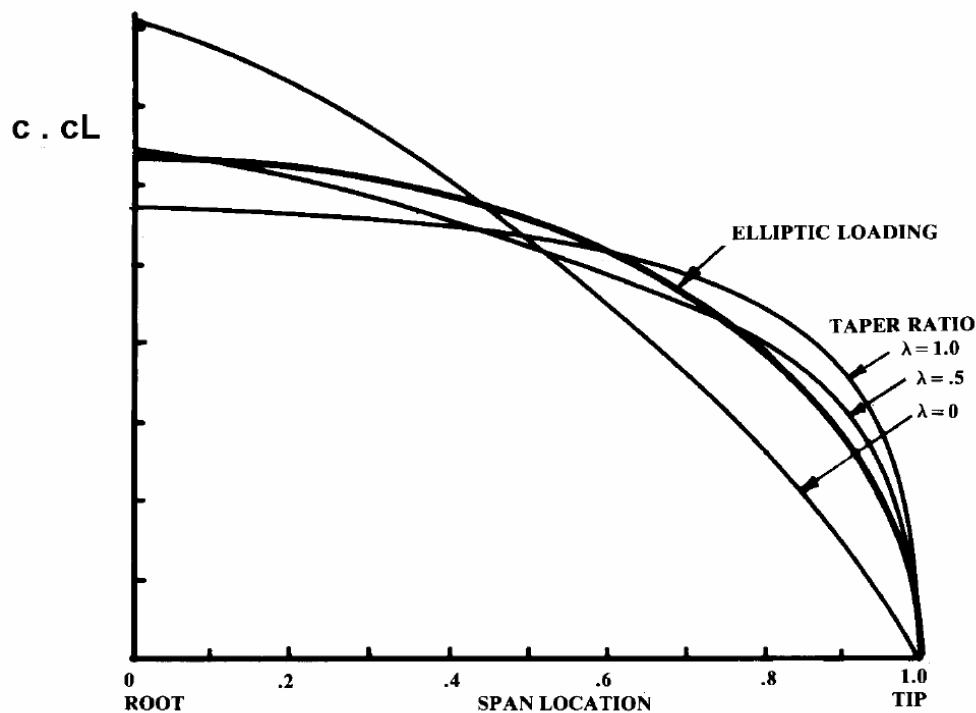


Figure 2.17 Lift distribution for various taper ratios (Raymer 2006, p.61)

On an untwisted wing the elliptical lift distribution (lowest induced drag) can be approximated by having a wing taper ratio defined by the following equation according to (Torenbeek 88).

$$\lambda_{\text{elliptical}} = 0.45 \cdot e^{-0.036 \cdot \Lambda_{.25}} \quad (2.17)$$

This equation is visual as the dotted line in Figure 2.18. The change in required taper ratio for elliptical lift distribution with changing the wing sweep can be explained by the fact that the airflow over a swept wing tends to divert from the free stream direction, which causes the lift distribution to change and thus requiring a different taper ratio to maintain an elliptical lift distribution.

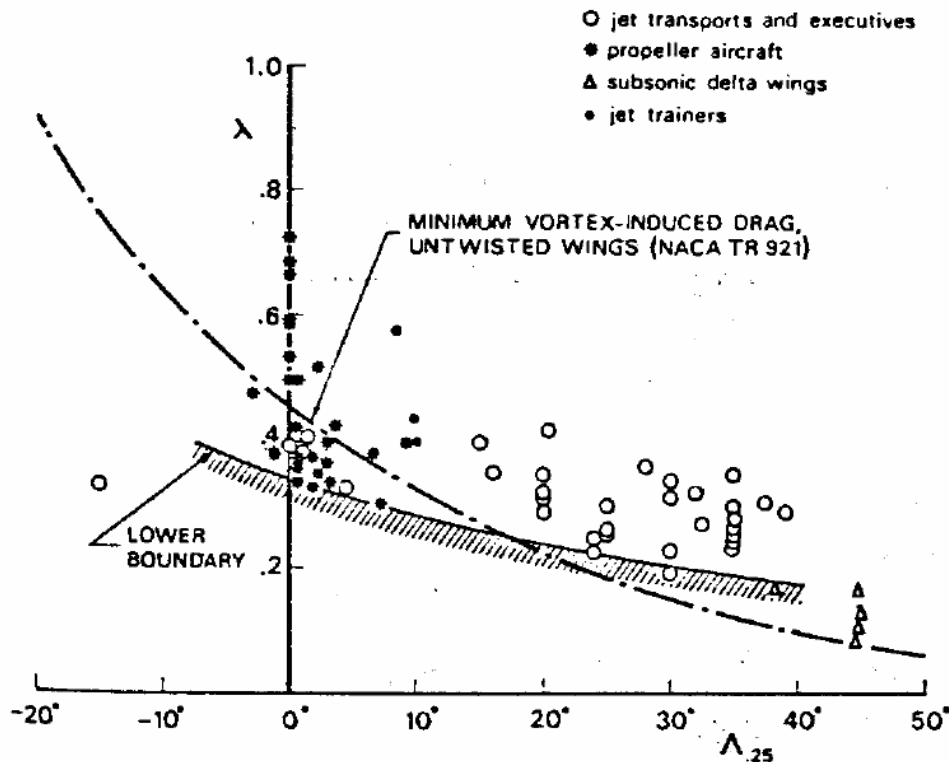


Figure 2.18 Taper ratios of straight, swept and delta wings (Torenbeek 1988)

Excessive Taper ratio on an untwisted wing causes the wingtip to stall first as can be seen in Figure 2.19. This causes an aft swept wing to generate a pitch-up moment, as the wing starts to stall. This causes the angle of attack to increase and leads to stalling of the entire wing. In combination with a T-tail configuration this can bring the aircraft in what is called a “deep stall”. Therefore taper ratios below 0.2 should be avoided.



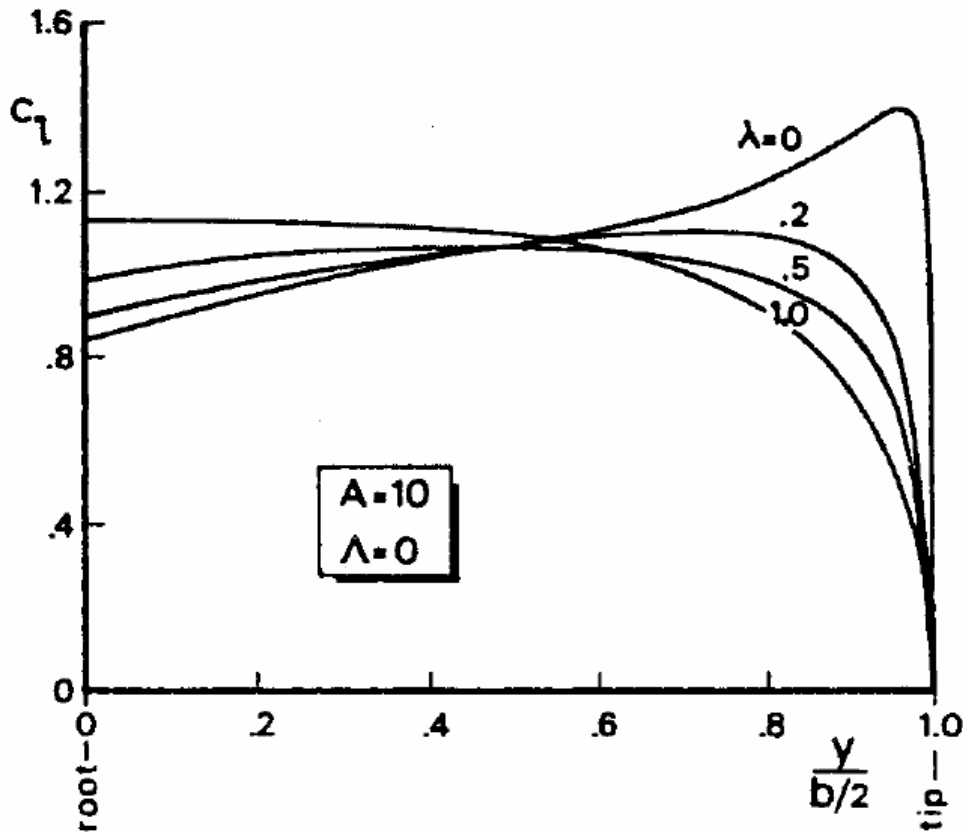


Figure 2.19 Section lift distribution on straight wings with various taper ratios (Torenbeek 1988)

Another problem with highly tapered wings is that the thickness of the tip is so reduced that it can cause mechanical difficulties for integration of the ailerons. This is the lower limit of wing taper given by (Howe 2000, p126)

$$\lambda = 0.2 \cdot A^{1/4} \cdot \cos(\Lambda_{25}) \quad (2.18)$$

A highly tapered wing has also some important advantages. The fuel tank volume is highest with a taper ratio of zero and the lift distribution approaches the weight optimum with low taper ratios. This effect can be seen if Figure 2.16 is compared with Figure 2.17. Therefore it is wise to choose the taper ratio not far above the lower limits suggested by the different authors.

### 2.5.3 Double tapered wing

For reasons of landing gear integration in a low wing configuration, the inner part of the wing trailing edge is sometimes unswept. This results in a different taper ratio for the inner part of the wing  $\lambda_i$  and the outer part of the wing  $\lambda_o$ . In this case we have a double trapezoid wing and the total wing taper ratio is the product of inner and outer taper ratio.

$$\lambda = \lambda_i \cdot \lambda_o \quad (2.19)$$

Another advantage of the higher root chord is that the absolute root thickness increases, which increases the bending resistance of the wing, resulting in a lighter wing.

The chord where the taper ratio of the wing changes is called the kink chord or  $c_k$ . The kink chord is usually defined as a ratio  $\eta_k$  which is defined as follows.

$$\eta_k = \frac{Y_k}{b/2} \quad (2.20)$$

The actual kink ratio is primarily defined by the landing gear integration, but as a good first estimation it should be something between 0.4 and 0.27 as can be seen for different aircraft in Table 2.3.

**Table 2.3** Kink ratios for different aircraft types (based on **Jane's 1997**)

aircraft type	$\eta_k$
<u>short range</u>	
B737 - 500	0.36
B737 - 900	0.29
A310	0.39
A320	0.37
<u>long range</u>	
A330	0.27
A340	0.27

Once the kink ratio is known we can calculate the kink span using equation 2.20 the areas of inner and outer trapezoid can be found with following equations.

$$S_i = (c_r + c_k) \cdot (Y_k - d_f / 2) \quad (2.21)$$

$$S_o = (c_k + c_r) \cdot (b/2 - Y_k) \quad (2.22)$$

In the tool the user can choose for a single tapered wing with one taper ratio or for a double tapered wing with both inner and outer taper ratio. Because the wing geometry drawing is based on the double tapered wing, it is necessary to calculate both inner and outer taper ratio if the user gives only the total wing taper ratio. The inner taper ratio can be found with following equation.

$$\lambda_i = \frac{(Y_k - d_f / 2) \cdot \lambda - Y_k + b/2}{b/2 - d_f / 2} \quad (2.23)$$

The outer taper ratio can be found using equation 3.4

For the total wing taper there are various suggestions:

- The elliptical lift distribution using equation 2.17.
- The lower limit according to (Howe 2000) using equation 2.18
- The lower limit according to (Torenbeek 1988) using an equation obtained through a regression on the line “lower boundary” in Figure 2.18. This is the equation which gives the lower limit according to (Torenbeek 1988).

$$\lambda_i = -0.0000012 \cdot 2\Lambda_{25}^3 + 0.00012348 \cdot \Lambda_{25}^2 - 0.00712927 \cdot \Lambda_{25} + 0.34347376 \quad (2.24)$$

All these suggestions are also combined in a graph which changes when the different parameters in the equation change. The graph can be seen in Figure 2.20.

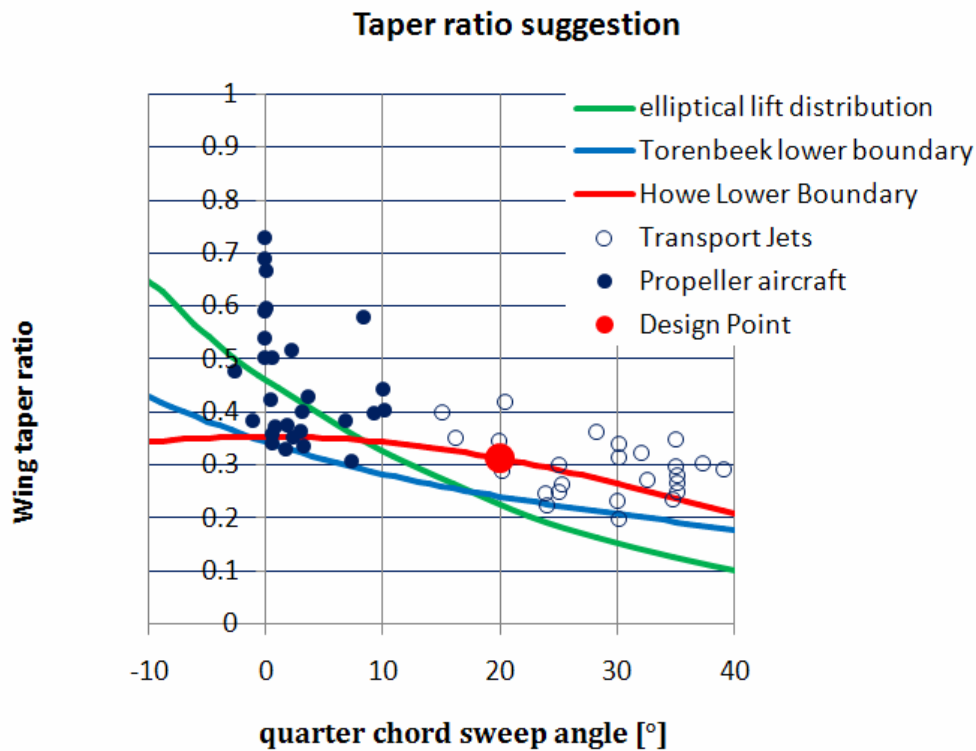


**Figure 2.20** Graph with various taper ratio suggestions as included in the tool

The chord lengths can be found using following equations.

$$c_k = \frac{S_{ref}}{\frac{d_f}{\lambda_i} + \frac{1}{(\lambda_i + 1)} \cdot \left( Y_k - \frac{d_f}{2} \right) + (1 + \lambda_o) \cdot \left( \frac{b}{2} - Y_k \right)} \quad (2.25)$$

$$c_r = \frac{c_k}{\lambda_i} \quad (2.26)$$

$$c_t = \lambda_o \cdot c_k \quad (2.27)$$

In the tool first the overall wing taper ratio has to be selected, as the literature suggestions always give this parameter. The next parameter required is the kink ratio, as this parameter selects how the wing should be split in both trapezoids. The kink ratio could also be defined during the sweep angle suggestion, but in that phase it does not have any influence on the selected sweep angles. As an early value 0.4 should be used for smaller aircraft; a lower value should be selected for larger aircraft.

6 lift distribution and chord distribution									
wing taper ratio	$\lambda$	<input type="text" value="0.270"/>	[-]	root chord	$c_r$	<input type="text" value="6.784"/>	[m]		
↑	Howe lower limit	<input type="text" value="0.27"/>	[-]	kink chord	$c_k$	<input type="text" value="4.070"/>	[m]		
↑	Torenbeek Lower limit	<input type="text" value="0.208"/>	[-]	tip chord	$c_t$	<input type="text" value="1.832"/>	[m]		
↑	elliptical spanloading	<input type="text" value="0.153"/>	[-]	kink semi-span	$Y_k$	<input type="text" value="7.33"/>	[m]		
				Aspect ratio inner trap	$A_i$	<input type="text" value="1.78"/>	-		
kink ratio	$\eta_k$	<input type="text" value="0.37"/>	[-]	Aspect ratio outer trap	$A_o$	<input type="text" value="8.46"/>	-		
				inner trap area	$S_i$	<input type="text" value="52.42"/>	[m <sup>2</sup> ]		
				outer trap area	$S_o$	<input type="text" value="73.66"/>	[m <sup>2</sup> ]		
				inside fuselage area	$S_f$	<input type="text" value="33.92"/>	[m <sup>2</sup> ]		
<input checked="" type="radio"/>	Inner Taper ratio	$\lambda_i$	<input type="text" value="0.600"/>	[-]	→	Outer Taper ratio	$\lambda_o$	<input type="text" value="0.450"/>	[-]
<input type="radio"/>	Outer Taper ratio	$\lambda_o$	<input type="text" value="0.400"/>	[-]	→	Inner Taper ratio	$\lambda_i$	<input type="text" value="0.675"/>	[-]
<b>select area's to be included in MAC calculation</b>				fuselage MAC	$c_{MAC,f}$	<input type="text" value="6.784"/>	[m]		
<input checked="" type="checkbox"/>	inside fuselage			fuselage MAC span	$Y_{MAC,f}$	<input type="text" value="1.250"/>	[m]		
<input checked="" type="checkbox"/>	inner trapezoid			inner MAC	$c_{MAC,i}$	<input type="text" value="5.540"/>	[m]		
<input checked="" type="checkbox"/>	outer trapezoid			inner MAC semi-span	$Y_{MAC,i}$	<input type="text" value="4.713"/>	[m]		
				outer MAC	$c_{MAC,o}$	<input type="text" value="3.093"/>	[m]		
				outer MAC semi-span	$Y_{MAC,o}$	<input type="text" value="12.780"/>	[m]		
				wing MAC	$c_{MAC}$	<input type="text" value="4.677"/>	[m]		
				wing MAC semi-span	$Y_{MAC}$	<input type="text" value="7.693"/>	[m]		

Figure 2.21 The thickness distribution as implemented in the tool.

## 2.6 Aerodynamic center of the wing

Since the wing consists of two trapezoidal surfaces we calculate the mean aerodynamic chord of each of the surfaces using equation 1.3. This yields for inner and outer trapezoid following formulas for the mean aerodynamic chord.

$$c_{MAC,f} = c_r \quad (2.28)$$

$$c_{MAC,i} = \frac{2}{3} \cdot c_r \cdot \frac{1 + \lambda_i + \lambda_i^2}{1 + \lambda_i} \quad (2.29)$$

$$c_{MAC,o} = \frac{2}{3} \cdot c_k \cdot \frac{1 + \lambda_o + \lambda_o^2}{1 + \lambda_o} \quad (2.30)$$

$$\text{With} \quad \lambda_i = \frac{c_k}{c_r} \quad (2.31)$$

$$\text{and} \quad \lambda_o = \frac{c_t}{c_k} \quad (2.32)$$

The MAC of the entire wing can now be calculated using following equation:

$$c_{MAC} = \frac{c_{MAC,f} \cdot S_f + c_{MAC,i} \cdot S_i + c_{MAC,o} \cdot S_o}{S_f + S_i + S_o} \quad (2.33)$$

The semi-span of the mean aerodynamic chord on an untwisted linearly tapered wing can be calculated equation 1.4. This equation gives the distance from the root chord to the MAC of the specific trapezoid. So in order to find the actual span-wise location of the MAC of this Trapezoid it has to be increased with the span-wise location of the root chord of the specific trapezoid. This yields for  $Y_{MAC,i}$  and  $Y_{MAC,o}$ :

$$Y_{MAC,f} = \frac{d_f}{4} \quad (2.34)$$

$$Y_{MAC,i} = \frac{d_f}{2} + \frac{1}{3} \cdot \left( y_k - \frac{d_f}{2} \right) \cdot \left( \frac{1 + 2\lambda_i}{1 + \lambda_i} \right) \quad (2.35)$$

$$Y_{MAC,o} = y_k + \frac{1}{3} \cdot \left( \frac{b}{2} - y_k \right) \cdot \left( \frac{1 + 2\lambda_o}{1 + \lambda_o} \right) \quad (2.36)$$

The span of aerodynamic chord of the entire wing  $Y_{MAC}$  can be found using the following equation:

$$Y_{MAC} = \frac{Y_{MAC,f} \cdot S_f + Y_{MAC,i} \cdot S_i + Y_{MAC,o} \cdot S_o}{S_f + S_i + S_o} \quad (2.37)$$

Now it is so that different manufacturers use different areas into account for the calculation of the MAC. In the tool there is an option included to choose which area(s) (inside fuselage area, inner trapezoid area and outer trapezoid area) the user wants to include in the calculation of the MAC. This is done by using multiplying each area  $S$  in equation (2.33) and (2.37) with a factor which equals 1 if the specific area has to be included and 0 if not.

The aerodynamic center of the entire wing for subsonic aircraft is located approximately at 25% of the MAC. For supersonic aircraft it moves backward to approximately 40% of the MAC. Since the tool is designed for subsonic aircraft only, the aerodynamic center in the tool is chosen at 25% of the MAC.

## 2.7 Incidence angle

The angle of attack of the wing during cruise flight is bound to the desired generated lift. There is a small variation in angle of attack as we can see on Figure 2.22, but in general we can say that it will approximate the mean cruise lift coefficient  $C_{L,C}$ . Since the wings are fixed the incidence angle will determine the angle of the cabin floor in respect to level floor during cruise flight.

Aerodynamically the fuselage should be tilted approximately  $3^\circ$  nose upward in order to generate the best lift to drag ratio for the fuselage. But in order to avoid excessive slope of the cabin floor (no more than  $2^\circ$  according to (Torenbeek 1988)).

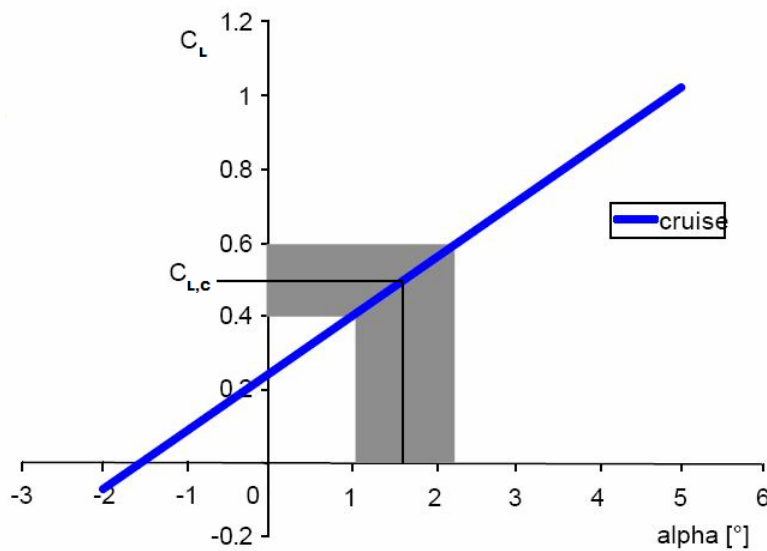


**Figure 2.22** Cruise wing lift coefficient range during cruise flight. (Böttger 2005)

The incidence angle can be calculated using following equation according to (Torenbeek 1988)

$$i_w = \frac{C_L^*}{C_{L_\alpha}} + \alpha_{0_t} \varepsilon_t + (\alpha_{l_0})_r \quad (2.38)$$

With:  $C_L^*$  = lift coefficient for which the fuselage reference line is horizontal.

$\alpha_{0_t}$  = change in zero lift angle of the wing per degree of positive twist at the tip

$(\alpha_{l_0})_r$  = zero lift angle at the root section



To get an initial value for the dihedral angle, we can use the guideline given in (Raymer 2006, p.65) or (Howe 2000) which can be seen in Table 2.4 and Table 2.5.

**Table 2.4** Dihedral guidelines (Raymer 2006, p.65)

Wing position and sweep	Low	Mid	High
Unswep	5 to 7	2 to 4	0 to 2
Subsonic swept wing	3 to 7	-2 to 2	-5 to -2
Supersonic swept wing	0 to 5	-5 to 0	-5 to 0

**Table 2.5** Dihedral guidelines (Howe 2000, p131)

Wing position and sweep	Low	High
Unswep	3 to 5	0
Swept back	3° at 30° aft sweep	-3° at 30° aft sweep

Since aft sweep increases lateral stability the effective dihedral angle needs to be reduced in order to maintain enough maneuverability with increased roll stability. Excessive dihedral effect produces a “Dutch roll”, a repeated side to side motion involving yaw and roll. To counter this effect, the vertical tail area needs to be increased, so it’s better to avoid excessive dihedral. A good guideline is that 10° of aft sweep reduces the dihedral angle by 1°. (Raymer 2006, p65)

In order to give an estimation including the actual value of the sweep angle and to give one exact value in every case, the table is modified using the following approximations.

- For the unswept (= sweep below 5° of sweep) wing we take the mean of the given range
- For swept wings we make sure that from 10 till 40° of sweep it stays in the range given in Table 2.4.
- 10° of positive (=aft) sweep equals -1° of dihedral.

The values used in the tool to give a suggestion according to (Raymer 2006) can be seen in Table 2.6.

**Table 2.6** Dihedral guidelines as used in the tool by (based on Raymer 2006, p.65)

Wing position and sweep	Low	Mid	High
Unswep	6	3	1
Subsonic swept wing	6*	2.5*	-1.5*

\*-1 deg for every 10 deg of aft sweep

The values used in the tool to give a suggestion according to (Howe 2000) can be seen in Table 2.7.

**Table 2.7** Dihedral guidelines as used in the tool by (based on Howe 2000, p.131)

Wing position and sweep	Low	High
Unswep	4	0
Subsonic swept wing	6*	0*

\*-1 deg for every 10 deg of aft sweep



In the tool, the wing twist angle can be given and is used for the calculation of the required incidence angle. The dihedral angle can also be chosen, in accordance with the suggestions given.

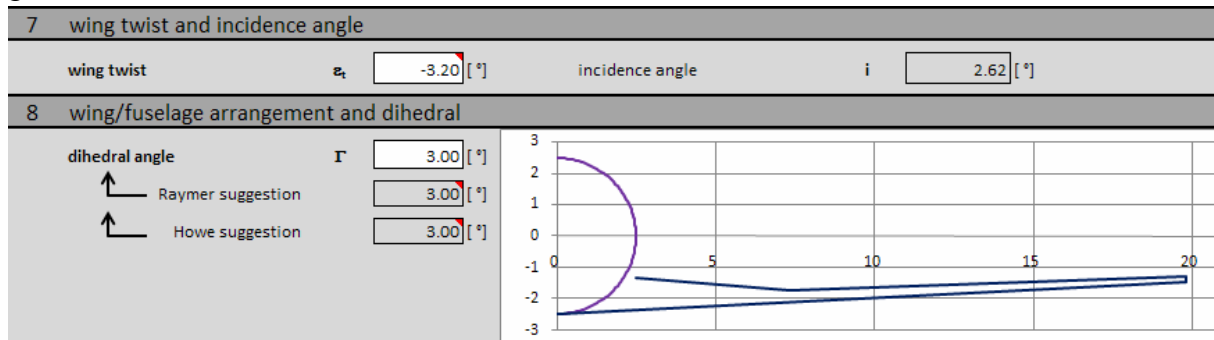


Figure 2.24 wing twist, incidence angle and dihedral angle

## 2.9 Wing control surfaces – ailerons

The outer part of the wing can generate extra lift or less lift (negative lift) in order to generate a moment around the longitudinal axis of the airplane, which is required to initiate a roll movement. This is generally obtained through simple flaps at the trailing edge of the outer wing, where the generated lift will exert the highest rolling moment. These flaps are especially designed to make symmetrical deflections and are called ailerons. Sometimes, when extra rolling moment is needed, spoilers can be used. They are located on the upper surface of the wing starting forward of the flaps till just aft the crest (position of maximum thickness). They spoil the airflow over the wing and disturb the lift generation. If deflected on one side of the aircraft, a roll moment is created.

### 2.9.1 Different types of ailerons

There are two types of ailerons, the first are low speed ailerons. These can be found on (almost) every aircraft. They are located on the outer part of the wing starting from about 50% till about 90% of the wing span. For larger aircraft (e.g. regional turboprops and transport jets) the ailerons occupy less of the wingspan, since they can be placed further outboard due to a higher wingspan and therefore the generated moment is increased thus resulting in a smaller aileron size. Actual guidelines, according to (Howe 2000, Table 8.2), can be found in Table 2.8. In general the relative size of the ailerons decreases with size and speed increase of the aircraft type.

Ailerons are usually tapered in chord by the same ratio as the wing and they usually cover 15 to 25% of the wing chord. On Figure 2.25 you can see a historical guideline concerning the relation between span and the chord of ailerons.

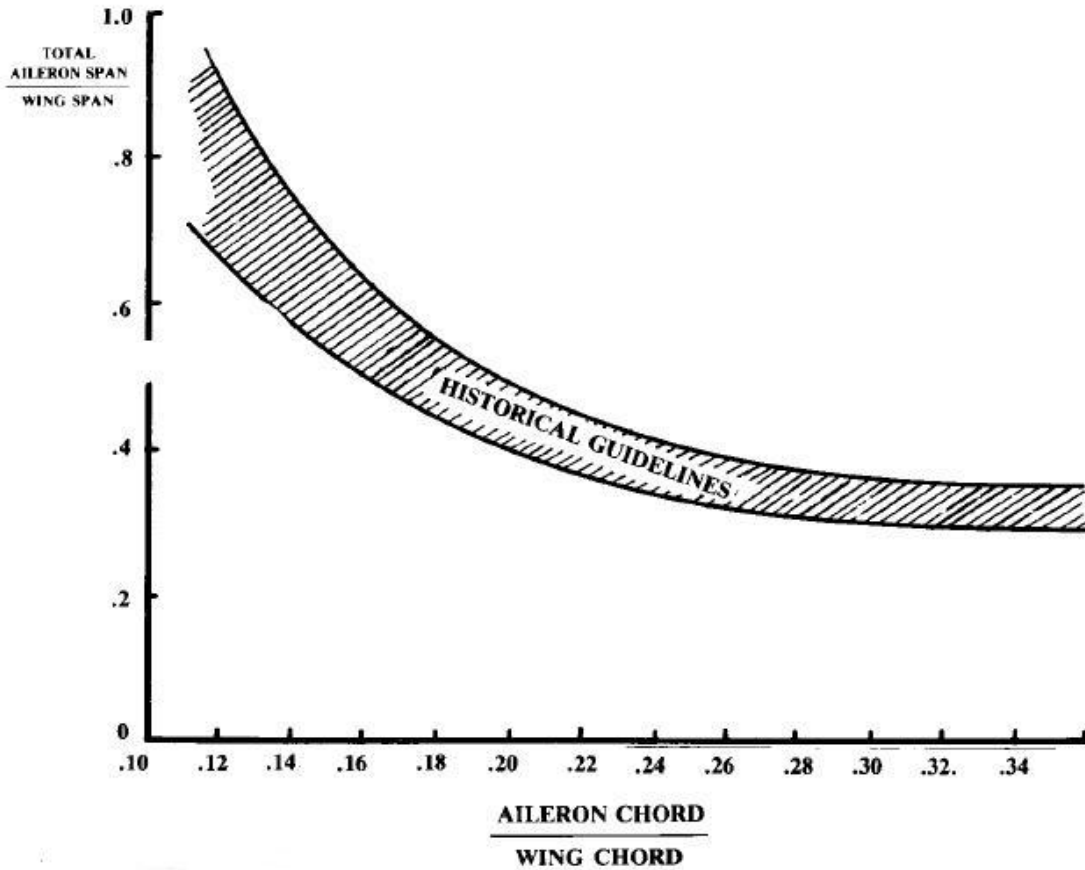


**Figure 2.25** Aileron chord and span guidelines (Raymer 2006, p124)

The high speed ailerons are the second type of ailerons, they can be found on many transport jets. At high speed, a deflected aileron can exert such a high force on the wing, that it twists the wing opposite to the desired roll direction. At some speed the generated twist rolling moment becomes so great that it exceeds the generated rolling moment by the aileron, thus reversing the rolling motion. To avoid this so called “aileron reversal”, many transport jets use an auxiliary, inboard aileron for high speed roll control, called the high speed ailerons.

### 2.9.2 Low speed aileron surface sizing

The aileron sizing used in the tool is based on the method used in (Howe 2000, p.256) a dimensionless parameter called the aileron volume coefficient  $V_A$ .

$$V_A = 0.5 \cdot \frac{S_A \cdot l_A}{S \cdot b} \quad (2.40)$$

$S_A$  = total area of all ailerons

$l_A$  = distance between the midpoints of the ailerons thus twice the span location ( $l_A = 2Y_{A,M}$ )

Typical values for aileron volume coefficient can be found in Table 2.8. These are used in the tool. Based on the type of aircraft, the aileron volume coefficient is chosen. Following from equation 2.40 the area and span-wise location can be traded. The span-wise location of the midpoint of the ailerons is described using a dimensionless parameter  $Y_{A,M}/b$ .

**Table 2.8** Aileron guidelines (Howe 2000, p127)

Aircraft type	High speed ailerons				Low speed ailerons				
	$b_A/b$	$c_A/c$	$y_{A,M}/b$	$S_A/S$	$b_A/b$	$c_A/c$	$y_{A,M}/b$	$S_A/S$	$V_A$
Twin prop general	-	-	-	-	0.320	0.260	0.360	0.065	0.024
twin regional turboprop	-	-	-	-	0.330	0.250	0.400	0.058	0.023
executive jets	-	-	-	-	0.270	0.250	0.390	0.052	0.020
jet transport	-	-	-	-	0.210	0.290	0.420	0.032	0.014
jet transport	0.08	0.23	0.19	0.02	0.200	0.230	0.430	0.026	0.014

Once the Aileron area  $S_A$  and the location of the midpoint  $Y_{A,M}$  are known, the chord-wise distribution  $c_A/c$  and span-wise distribution  $b_A/b$  have to be traded (since the area is already fixed) using following equation.

$$S_A = \left(\frac{c_A}{c}\right) \cdot \left(\frac{b_A}{b}\right) \cdot b \cdot c_k \cdot \left(1 - \frac{1 - \lambda_o}{b/2 - Y_k} \cdot (Y_{A,M} - Y_k)\right) \quad (2.41)$$

Another good guideline is Figure 2.25 where you can graphically see the trade off between aileron chord and span.

### 2.9.3 Aileron geometry

With these four aileron parameters selected, the aileron geometry is entirely described and other geometric aileron properties can be calculated. The inner and outer chord span can be calculated as follows.

$$Y_{r,A} = Y_{A,M} - \left(\frac{b_A}{b}\right) / 4 \quad (2.42)$$

$$Y_{l,A} = Y_{A,M} + \left(\frac{b_A}{b}\right) / 4 \quad (2.43)$$

$b_A/b$  has to be divided by four because  $b_A$  includes both ailerons. The inner and outer chord length can be derived from:

$$c_{r,A} = c_k \cdot \left(1 - \frac{1 - \lambda_o}{b/2 - Y_k} \cdot (Y_{r,A} - Y_k)\right) \quad (2.44)$$

$$c_{t,A} = c_k \cdot \left( 1 - \frac{1 - \lambda_o}{b/2 - Y_k} \cdot (Y_{t,A} - Y_k) \right) \quad (2.45)$$

Finally this yields for the Mean aerodynamic chord length and span.

$$c_{MAC,A} = \frac{2}{3} \cdot c_{A,i} \cdot \left( \frac{1 + (c_{t,A}/c_{r,A}) + (c_{t,A}/c_{r,A})^2}{1 + (c_{t,A}/c_{r,A})} \right) \quad (2.46)$$

$$Y_{MAC,A} = Y_{r,A} + \frac{1}{3} \cdot (Y_{t,A} - Y_{r,A}) \cdot \left( \frac{1 + 2 \cdot (c_{t,A}/c_{r,A})}{1 + (c_{t,A}/c_{r,A})} \right) \quad (2.47)$$

## 2.9.4 High speed aileron surface sizing

A first estimation of the high speed ailerons is based on Table 2.8, although the aileron volume coefficient cannot be used, because the value is given for both ailerons together, thus resulting in a total area of both ailerons together. Therefore the trade between aileron area and midpoint span cannot be used (for both high and low speed ailerons) if we include high speed ailerons. The area of both the aileron sets is determined using the guideline for  $S_A/S$ .

$$S_A = \left( \frac{S_A}{S} \right) \cdot S \quad (2.48)$$

$$S_{A,H} = \left( \frac{S_{A,H}}{S} \right) \cdot S \quad (2.49)$$

As the high speed ailerons are located in the kink location, the aileron can be located in both the trapezoids of the wing. The calculation of the inner and outer chord length is therefore dependent upon their exact span-wise location. So the length of a chord at a certain location  $Y_x$  can be determined using:

- For  $Y_x < Y_k$  
$$c_x = c_r \cdot \left( 1 - \frac{1 - \lambda_i}{Y_k - d_f/2} \cdot (Y_x - d_f/2) \right) \quad (2.50)$$

- For  $Y_x > Y_k$  
$$c_x = c_k \cdot \left( 1 - \frac{1 - \lambda_o}{b/2 - Y_k} \cdot (Y_x - Y_k) \right) \quad (2.51)$$

If the inner and outer chord of the high speed aileron are located both in one trapezoid one might think that the ailerons trailing edge will have a kink. This is solved by considering the aileron as one trapezoid between the inner and outer chord.

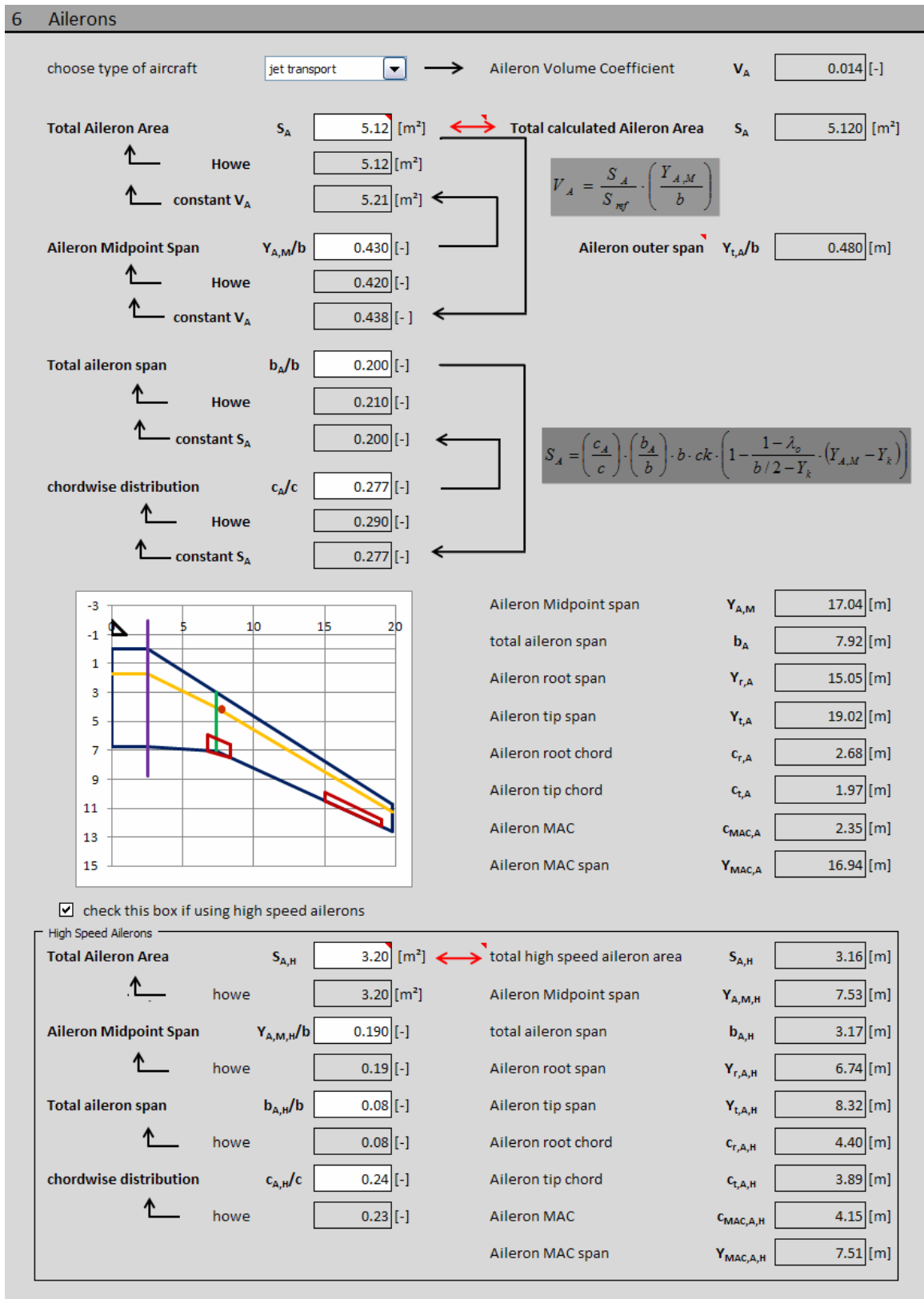


Figure 2.26 Aileron design as implemented in the tool

This difficulty in calculating the chord lengths of the aileron resulted also in the loss of the trade of between aileron chord and span, because there is no general equation for the area of the aileron depending on only chord and span of the aileron. Therefore both the values have to

be selected so that the calculated aileron area is approximately the same as the estimated aileron area from the guidelines in Table 2.8. In Figure 2.26 one can see in row 185 the two cells of aileron area, if both differ more than 5%; the right cell will turn red.

All other equations derived for low speed ailerons remain valid for the high speed ailerons.

In the tool, the same way is followed as suggested above; this can be seen in Figure 2.26.

## 2.10 Lift predictions of the wing

Now that the main wing geometry has been defined, it is possible to make some early aerodynamic estimations concerning the lift coefficient of the entire wing  $C_L$  and the lift gradient  $C_{L\alpha}$  of the entire wing.

### 2.10.1 Wing lift gradient.

The first parameter we calculate is the lift gradient  $C_{L\alpha}$ . This parameter is required during the conceptual design for three reasons:

- For properly setting the wing incidence angle (see paragraph 2.7)
- For the calculation for the drag due to lift. (Later in the conceptual design)
- For longitudinal stability analysis. (Later in the conceptual design)

The lift gradient of the wing can be calculated using following equation (Raymer 2006, p.311)

$$C_{L\alpha} = \frac{2\pi \cdot A}{2 + \sqrt{4 + \frac{A^2 \cdot \beta^2}{\eta^2} \left(1 + \frac{\tan^2 \Lambda_{\max t}}{\beta^2}\right)}} \cdot \left(\frac{S_{\text{exposed}}}{S_{\text{ref}}}\right) \cdot F \quad (2.52)$$

$S_{\text{exposed}}$  is the area of the wing top view which is located outside the fuselage.

$\Lambda_{\max t}$  is the sweep of the wing at the chord location where the airfoil is thickest.

$$\beta^2 = 1 - M^2 \quad (2.53)$$

$$\eta = \frac{C_{l\alpha}}{2\pi/\beta} \quad (2.54)$$

F is the fuselage lift factor and can be calculated as follows:

$$F = 1.07 \cdot \left(1 + \frac{d_f}{b}\right)^2 \quad (2.55)$$

The product  $(S_{\text{exposed}}/S_{\text{ref}}) \cdot F$  can be greater than one, implying that the fuselage produces more lift than the portion of the wing it covers, this is unlikely; therefore we take 0.98 as maximum value for this product.

For implementation in the tool equation (2.52) requires an input value of  $C_{l\alpha}$  and  $\Lambda_{\text{max}l}$ . Since the airfoil has already been selected, these values should be known to the user.

If however the airfoil has not yet been selected, then the user can chose to not include these parameters in the calculation of the lift gradient, thus resulting in these assumptions:

- $\eta = 0.95$  for all Mach numbers (**Raymer 2006**, p.312)
- $\Lambda_{\text{max}l} = \Lambda_{50}$

This gives a simplified form of equation (3.5)

$$C_{L\alpha} = \frac{2\pi \cdot A}{2 + \sqrt{4 + (A/0.95)^2 (1 + \tan^2 \Lambda_{50} - M^2)}} \cdot \left(\frac{S_{\text{exposed}}}{S_{\text{ref}}}\right) \cdot F \quad (2.56)$$

### 2.10.2 Maximum clean wing lift coefficient

The maximum lift coefficient of the entire wing without extended flaps or slats can be calculated using equation (2.57) (**Raymer 2006**, p.316)

$$C_{L,\text{max},\text{clean}} = 0.9 \cdot C_{l,\text{max}} \cdot \cos \Lambda_{25} \quad (2.57)$$

More detailed estimations of maximum wing lift can be found in (**Raymer 2006**, paragraph 12.4) or in (**DATCOM 1978**).

### 2.10.3 Maximum wing lift coefficient with high lift devices

The total maximum wing lift in landing configuration will be the sum of the clean wing lift coefficient and the wing lift increment due to high lift devices.

$$C_{L,max,highlift} = C_{L,max,clea} + \Delta C_{L,max} \quad (2.58)$$

$\Delta C_{L,max}$  Is explained the next paragraph (2.11).

## 2.11 High lift devices

The main goal of high lift devices is increasing the maximum lift coefficient of the wing during Take off and Landing in order to meet the required take off and landing lift coefficients  $C_{L,TO}$  and  $C_{L,L}$ .

During take off it is also important to have an optimum lift to drag ratio, because this reduces the required take off thrust, which is one of the determining factor in the maximum required thrust estimation (See matching chart). During landing it is more important to have a high drag in order to reduce the lift to drag ratio so that a high descent angle can be achieved.

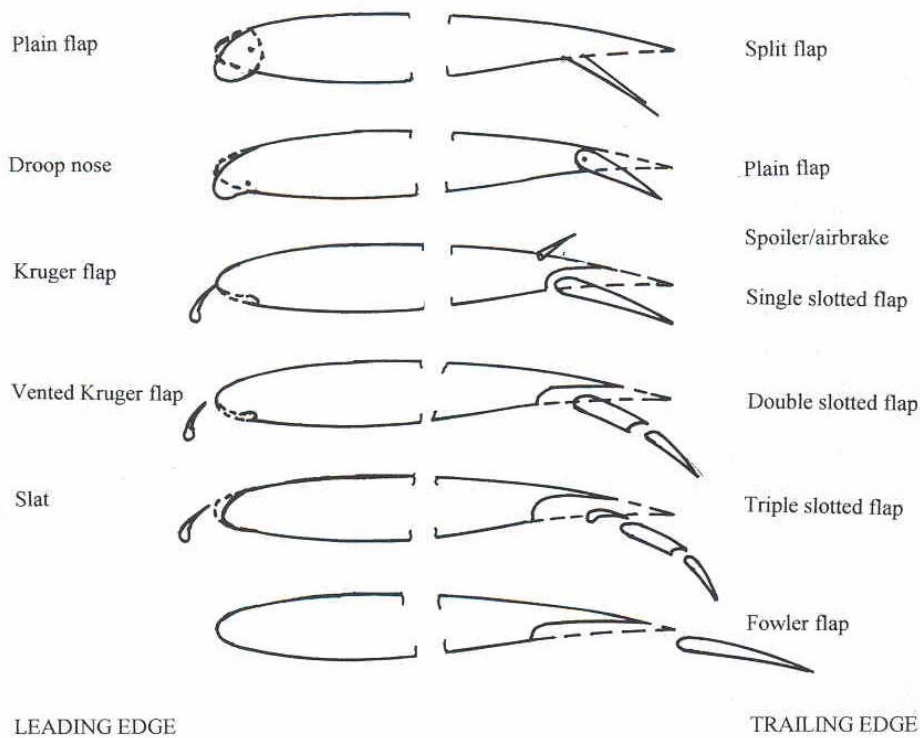


**Figure 2.27** Different types of high lift devices (Howe 2000, Figure 5.2)

It is always advised to use the most “simple” system (e.g. no triple slotted flaps, no slats...) that generates the required lift during take off and landing. The different types of high lift devices can be seen in Figure 2.27. In (Raymer 2006, p.321) a brief description of the advantage of every type of high lift device is given.



The increase of the maximum lift of the airfoil due to high lift devices is called  $\Delta c_l$ . This is the increase of the airfoil in 2D flow regime. Values for this increase should be obtained from test data of the selected airfoil. If however no test data is available, approximations from Table 2.9 can be used.

**Table 2.9** High lift device efficiency (Howe 2000, p123)

Type of high lift device	$\Delta c_l (2D)$	%c
<b>Leading edge</b>		
Plain flap	0.5	15
Vented slat	1.0	18
Kruger flap	0.8	20
vented Kruger flap	1.0	20
<b>Trailing edge</b>		
Plain Flap	0.8 – 1.10	20 - 40
Split Flap (no gap)	0.9 – 1.4	20 - 40
single-slotted flap	1.2 – 1.8	20 - 40
Double-slotted flap	2.5	40
Triple-slotted flap	2.9	40
Fowler flaps	1.2 – 1.8	20 - 40
Fowler plus split flap	2.2	40

For chord lengths between the ones given in Table 2.9 a linear interpolation between the maximum and minimum value for lift coefficient is made.

The increase in total wing lift due to high lift devices can be estimated according to (Raymer 2006, p.326) using this equation.

$$\Delta C_{L,\max} = 0.9 \cdot \Delta c_{l,\max} \cdot \left( \frac{S_{flapped}}{S_{ref}} \right) \cos \Lambda_{HL} \quad (2.59)$$

With  $\Lambda_{HL}$  is the sweep back angle of the hinge line of the flap. In the tool this will be approximated as the leading edge of trailing edge high lift devices and the trailing edge of leading edge high lift devices.

$S_{flapped}$  is the flapped wing area; this is the wing area in which the airfoil sections are affected by the high lift device. A definition can also be seen in Figure 2.28.

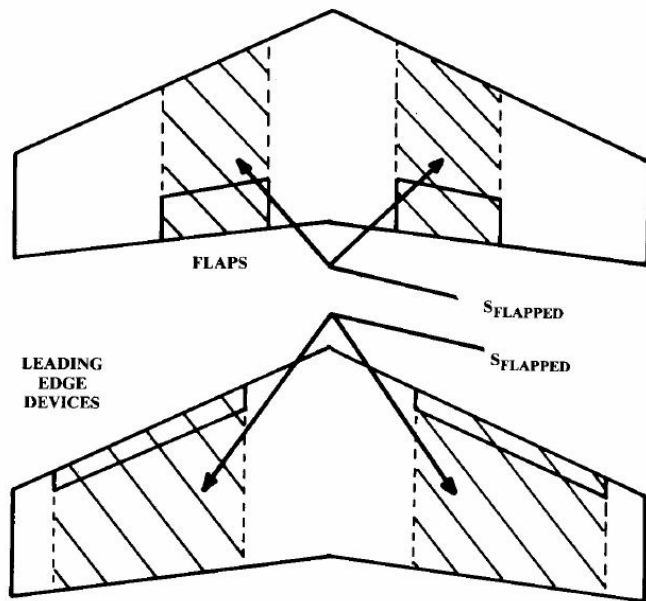


Figure 2.28 Definition of flapped wing area (Raymer 2006, p327)

10 high lift devices

select leading edge high lift devices

Chordwise distribution  $c_{HL,LE}/c$   [%]  
 ↑ Howe  [%] LE high lift tip semi-span  $Y_{HL,LE,t}$   [m]  
 LE high lift tip semi-span ratio  $Y_{HL,LE,t}/b$   total LE high lift span  $b_{HL,LE}$   [-]  
 ↑ howe  [-]  
 Airfoil lift increase  $\Delta C_{L,LE}$   [-] Wing lift increase  $\Delta C_{L,LE}$   [-]  
 ↑ Howe

select trailing edge high lift devices

Chordwise distribution  $c_{HL,TE}/c$   [%] total TE high lift span  $b_{HL,TE}$   [-]  
 ↑ howe  [%]  
 Airfoil lift increase  $\Delta C_{L,TE}$   [-] Wing lift increase  $\Delta C_{L,TE}$   [-]  
 ↑ howe  [-]

Maximum wing lift coefficient check: make sure that the calculated maximum wing lift coefficient is sufficient

Take off lift coefficient  $C_{L,TO}$   < total wing Max lift coeff  [-]  
 Landing lift coefficient  $C_{L,L}$

Figure 2.29 High lift device selection in the tool.

The high lift device selection in the tool can be seen in Figure 2.29. The calculated maximum wing lift coefficient with high lift devices extended has to be higher than the values needed for

According to (Raymer 2006, p.326) the wing lift coefficient in take off configuration will be 60 to 80% of the one in landing configuration; in the tool is chosen for 80%. If these requirements are not fulfilled, the square of the calculated total maximum wing lift coefficient will turn red in order to warn the user.

## 2.12 Fuel tank estimation

After the wing geometry is defined we can make a rough estimation of the fuel tank volume. We assume the room between the two wing spars as the fuel tank; with some correction factors the first estimation gives a good prediction.

A good estimation of the fuel tank volume according to (Torenbeek 1988) is determined with the following equation:

$$V_{Tank} = 0.54 \cdot S_{Ref}^{1.5} \cdot (t/c)_r \cdot \frac{1}{\sqrt{A}} \cdot \frac{1 + \lambda \cdot \sqrt{\tau} + \lambda^2 \cdot \tau}{(1 + \lambda)^2} \quad (2.60)$$

This equation has been applied to the inner and outer wing separately leading to inner  $V_{F,I}$  and outer  $V_{F,o}$  fuel tank volume. Therefore we have to use the parameters of the inner or outer trapezoid in equation 2.58 to calculate these inner and outer fuel tanks volumes.

This equation has a maximum error of 10%. Thus the maximum required fuel volume, calculated during the preliminary sizing, should not be higher than the calculated tank volume reduced with 10 percent. If in the tool, as can be seen in Figure 2.30, the required margin is not fulfilled, there will be a message to the user. In the left bottom part the used fuel tanks can be selected; the inboard fuel tank can be chosen feely.

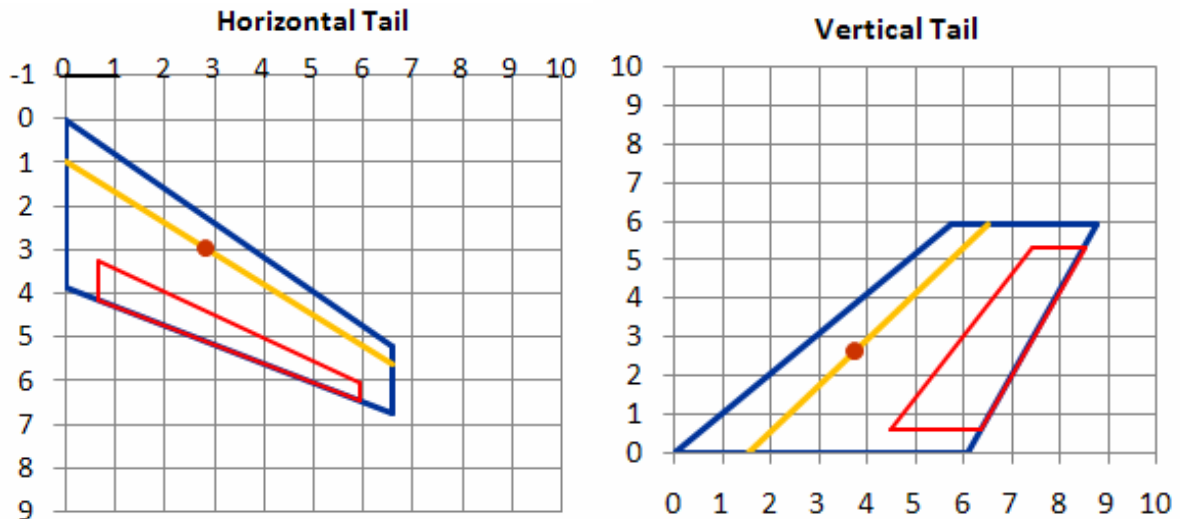
11 fuel tank volume estimation			
Required fuel mass	$M_F$	<input type="text" value="26000.00"/>	[kg]
fuel density	$\rho_F$	<input type="text" value="800.00"/>	[kg/m <sup>3</sup> ]
<u>Select used fuel tanks</u>			
<input checked="" type="checkbox"/>	Outer wing fuel tank	$V_{FI}$	<input type="text" value="9.04"/>
<input checked="" type="checkbox"/>	inner wing fuel tank	$V_{Fo}$	<input type="text" value="15.53"/>
<input type="checkbox"/>	Inboard fuel tank	$V_{FF}$	<input type="text" value="10.00"/>
	total fuel tank	$V_F$	<input type="text" value="24.57"/>
	Total calculated fuel mass	$M_{FC}$	<input type="text" value="19656"/>
	fuel mass fraction	$m_F/m_{MTO}$	<input type="text" value="0.20"/>
<b>Wing fuel volume not sufficient</b>			

Figure 2.30 Fuel tank volume estimation in the tool.

### 3 Conceptual design of the empennage

The empennage's function is to rotate and balance the aircraft around its center of gravity. This is done by generating lifting forces at a distance from the center of gravity. In this chapter a first estimation of the size and geometry of the empennage is made, based on statistics of previously designed aircraft. The different steps followed in the tool are:

1. Input data from earlier design phases
2. General arrangement, position and size of the empennage.
3. Horizontal tail geometry
4. Vertical tail geometry
5. Elevator
6. Rudder
7. Stall and spin recovery



**Figure 3.1** Horizontal and vertical tail as described in the tool.

After all the parameters are selected, the vertical and horizontal tail are described as can be seen in Figure 3.1.

### 3.1 General empennage configurations

There are various tail geometries which can fulfill the required control upon the aircraft, but it is beyond the scope of this thesis to include all of them. Therefore the most appropriate (and conventional) for subsonic aircraft have been included in the tool. Figure 3.2 gives an example of the included tail geometries

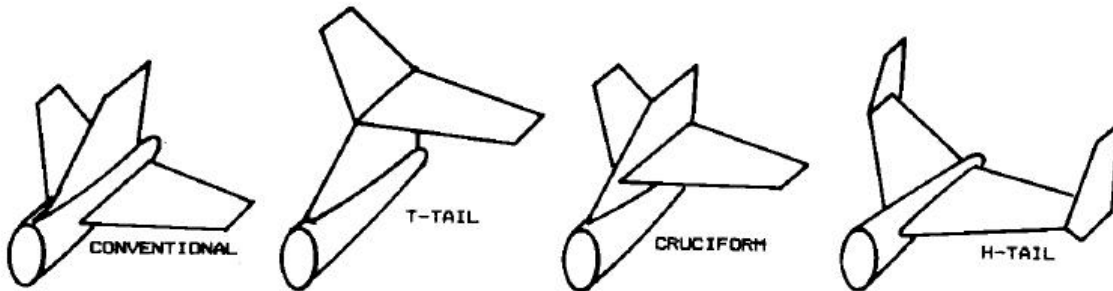


**Figure 3.2** Different empennage configurations (**Raymer 2006**, Figure 4.30)

The effect of the different configurations is taken into account for using a so called equivalent tail volume coefficient, which is basically a factor describing the efficiency of a certain tail configuration efficiency compared to the efficiency of a conventional tail and is discussed in paragraph 3.2 and can be seen in Table 3.3.

In general we can say that the T-tail is more efficient than the conventional tail because of the “end plate effect”, as like a winglet on a wingtip. But with the T-tail configuration there is the risk to come in a state of deep stall, where it is impossible to recover. Another drawback is the weight penalty because of higher required vertical tail strength. The H-tail has the advantage of the end plate effect only on the horizontal tail, but has a weight penalty due to the placement of the vertical tail planes on the horizontal tail. For more information on the tail arrangement see (**Raymer 2006**, paragraph 4.5).

### 3.2 Surface size of the empennage

The initial layout of the empennage is done using a historical approach. The moment created by the empennage around the center of gravity of the aircraft is proportional to the lifting force and the lever arm of the empennage. Since the primary purpose of a tail is to counteract moments produced by the wing, the size of the empennage is related to the size of the wing.

The lifting forces of the empennage are related to its surface the effectiveness of the empennage (to create moments around the center of gravity) can now be described as the product of its surface and its lever arm. In order to relate this “effectiveness” to the size of the aircraft, we divide by the wing surface.

Rendering this parameter dimensionless requires dividing by some quantity of length. For the **vertical tail** the, the wing yawing moments which must be countered are most directly related to the wing span  $b$ . this leads to the vertical tail volume coefficient:

$$C_V = \frac{S_V \cdot l_V}{S_W \cdot b} \quad (3.1)$$

For a **horizontal tail** or a canard the pitch moments which must be countered are most directly related to the Mean aerodynamic chord of the wing  $c_{MAC}$ . This leads to the horizontal tail volume coefficient:

$$C_H = \frac{S_H \cdot l_H}{S_W \cdot c_{MAC}} \quad (3.2)$$

The lever arms are defined as the distance in longitudinal direction between the centers of lift for the surfaces. Since we work with subsonic aircraft the center of lift is near to 25% of the MAC of the lifting surface. (**Raymer 2006**, p.53) The lever arms and surfaces are also defined in Figure 3.3 according to (**Corke 2003**).

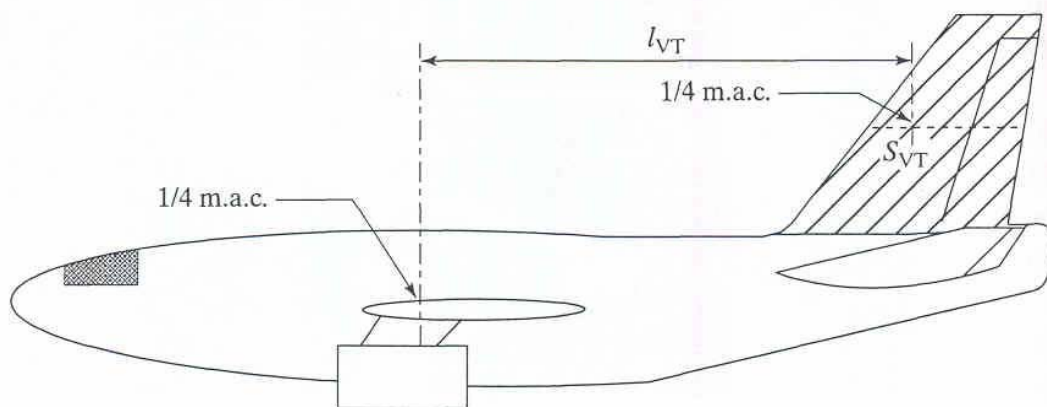
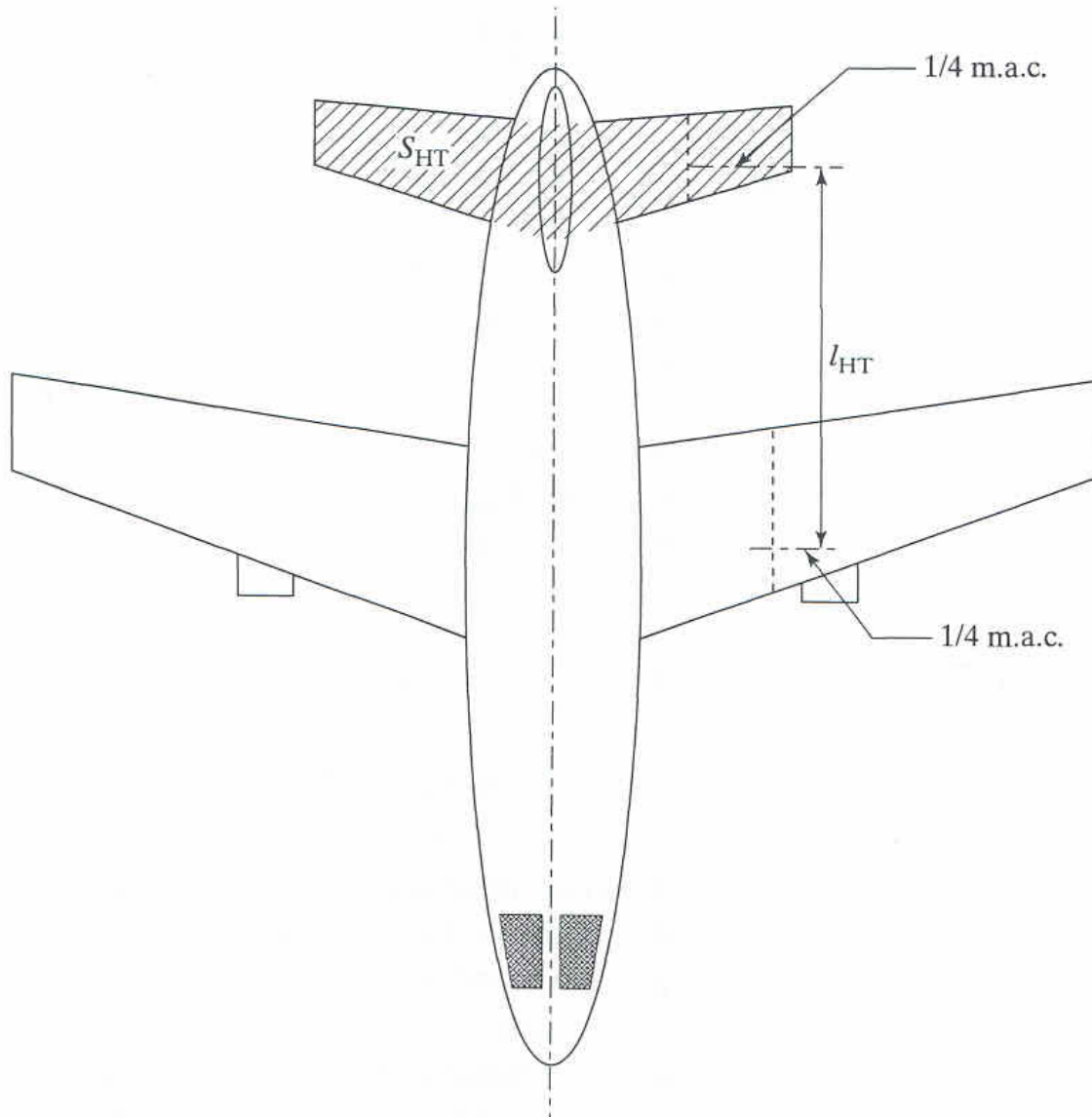


**Figure 3.3** Definition of empennage surfaces and lever arms (Corke 2003)

According to (Raymer 2006, p122) typical values for the tail volume coefficients for different aircraft can be found in Table 3.1.

**Table 3.1** Tail volume coefficients (Raymer 2006, p.122)

Aircraft type	$C_H$	$C_V$
twin turboprop	0.90	0.08
Transport Jets	1.00	0.09

The only thing which remains unknown to calculate the area of the vertical and horizontal tail is the lever arm. The position of the vertical and horizontal tail depends on the position of the center of gravity, but in order to calculate the position of the center of gravity, the position of the vertical and horizontal tail is required; this problem can only be solved through an iterative process. For the first estimation however we can use historical guidelines based upon the installation of the engines seen in Table 3.2.

**Table 3.2** First lever arm estimation (Raymer 2006, p.123)

configuration	$l_H/l_F$ and $l_V/l_F$
engines on the wing	0.50 - 0.55
engines on the tail (fuselage)	0.45 - 0.50

The formula for the vertical and horizontal tail area as used in the tool result from equations (4.1) and (4.2)

$$S_V = \frac{C_V \cdot S_W \cdot b}{l_V} \quad * \quad (3.3)$$

$$S_H = \frac{C_H \cdot S_W \cdot c_{MAC}}{l_H} \quad (3.4)$$

\*The vertical tail area does not include the area inside the fuselage in the contrary to the definition of the horizontal tail area. (Corke 2003, paragraph 6.2.1)

In certain cases (e.g. different configurations, all moving tail...) the original volume coefficient can be reduced. This is included by relating an equivalent tail volume coefficient to each configuration, by which the original tail volume coefficient has to be multiplied. The different influences are described below and are summarized in Table 3.3.

- For an all moving tail, the tail volume coefficients can be reduced by about 10%.
- For an aircraft with a computerized active flight control system, the tail volume coefficients may be reduced by approximately 10% provided that trim, engine-out, and nose wheel liftoff requirements can be met. (Raymer 2006, p.123)
- For a T-tail configuration the vertical and horizontal tail coefficients can be reduced by 5% compared to a conventional tail, because of the end plate effect.



- For an H-tail configuration, the horizontal tail volume coefficient can be reduced by 5% because of the end plate effect. The vertical tail area on each side will be one-half of the required total area corresponding to a conventional tail.
- For a V-tail design, theoretically the required total area is smaller than with a conventional configuration, but experimental research has shown that the advantage gets lost in the inefficiency of the V-tail configuration. The total surface area needed with a V-tail is therefore the same as the total horizontal and vertical tail area needed as with a conventional configuration.

$$S_{V-Tail} = S_V + S_H \quad (3.5)$$

The V-angle  $\nu$  between the two surfaces is determined by:

$$\nu_{V-Tail} = 2 \cdot \tan^{-1} \left( \sqrt{\frac{S_V}{S_H}} \right) \quad (3.6)$$

This angle should be about 90°

**Table 3.3** Equivalent Tail volume coefficients for different configurations (based on **Raymer 2006**, p.123 **Corke 2003**, p.126)

Empennage configuration	Equivalent $C_V$	Equivalent $C_H$
All moving Tail	0.90*	0.90*
“Computerized Active Flight control system”	0.90	0.9
H-Tail	0.50	0.95
T-Tail	0.95	0.95
V-Tail	1.00	1.00

\*Only applicable on the tail surface which is all moving.

Empennage design					
Input data from earlier design phases					
wing area	$S_{ref}$	<input type="text" value="160"/>	[m <sup>2</sup> ]		
Wing MAC	$C_{MAC}$	<input type="text" value="4.68"/>	[m]		
Wing Span	b	<input type="text" value="39.62"/>	[m]		
Fuselage length	$f_l$	<input type="text" value="40.00"/>	[m]		
	↑ Estimation based on MTOW	<input type="text" value="40.54"/>	[m]		
Cruise Mach number	$M_c$	<input type="text" value="0.85"/>	[-]	drag divergence numb	$M_{DD,E}$ 0.90 [-]
general arrangement, position and size of the empennage					
select aircraft type	<input type="text" value="Transport Jets"/>				
select engine configuration	<input type="text" value="engines on the wing"/>		vertical tail volume coeff	$C_H$	<input type="text" value="1.00"/>
select empennage configuration	<input type="text" value="conventionnal"/>		horizontal tail volume coeff	$C_V$	<input type="text" value="0.090"/>
lever arm Hor tail	$l_H$	<input type="text" value="21.00"/>	[m]		
	↑ Raymer suggestion	<input type="text" value="21.00"/>	[m]		
lever arm Vert tail	$l_V$	<input type="text" value="21.00"/>	[m]		
	↑ Raymer suggestion	<input type="text" value="21.00"/>	[m]		
<u>select other tail properties</u>					
	<input type="checkbox"/>	all moving Horizontal tail			
	<input type="checkbox"/>	all moving Vertical tail			Horizontal tail area
	<input type="checkbox"/>	computerized active flight control			$S_H$ <input type="text" value="35.64"/>
				Vertical tail area	$S_V$ <input type="text" value="27.17"/>

**Figure 3.4** Input data, general arrangement and surface sizing of the empennage.

In the upper part of Figure 3.4 input data from earlier design phases has to be given. This part has been included in order to make it possible for the user to design an empennage, without going through the previous design sheets. Normally, these values are automatically taken from the previous sheets, so they don't have to be given by the user.

The second part of Figure 3.4 gives the first estimation of empennage areas; this requires input data concerning general arrangement of the empennage as described above in paragraph 3.2.

### 3.3 Geometry selection

#### 3.3.1 Wing shape

Once the required areas are known, the top view geometry of the empennage has to be determined. This is done the same way as a single trapezoidal wing. As the empennage size is related to wing size, other geometric parameters are also related to the wing. A first estimation of the geometric parameters of the empennage can be done using Table 3.4 to Table 3.6; these values are based on previous aircraft designs.

**Table 3.4** Horizontal tail geometry guidelines (**Roskam II 1985**)

Aircraft type	$\Gamma_h [^\circ]$	$i_h [^\circ]$	$A_h$	$\Lambda_h [^\circ]$	$\lambda_h$
regional turboprop	0 - 12	0 - 3 fix/variable	3.4 - 7.7	0 - 35	0.39 - 1.0
business jet	-4 - 9	-3.5	3.2 - 6.3	0 - 35	0.32 - 0.57
Transport jet	0 - 11	variable	3.4 - 6.1	18 - 37	0.27 - 0.62

**Table 3.5** Vertical tail geometry guidelines (**Roskam II 1985**)

Aircraft type	$\Gamma_v [^\circ]$	$A_v$	$\Lambda_v [^\circ]$	$\lambda_v$
regional turboprop	90	0.8 - 1.7	0 - 45	0.32 - 1
business jet	90	0.8 - 1.6	28 - 55	0.30 - 0.74
Transport jet	90	0.7 - 2.0	33 - 53	0.26 - 0.73

**Table 3.6** Empennage guidelines (**Howe 2000**, p.255)

geometry suggestion	$A$	$\Lambda/\Lambda_{wing}$	$\lambda/\lambda_{wing}$
horizontal tail	$(0.5 \text{ to } 0.6) \cdot A_{Wing}$	1	1.2
Vertical Tail	1.2 to 3	1*	0.5

\*usually not less than 20° of quarter chord sweep.

Once aspect ratio is selected a calculation of the span can be done using following equations.

$$b_H = \sqrt{A_H \cdot S_H} \quad (3.7)$$

$$b_V = \sqrt{A_V \cdot S_V} \quad (3.8)$$

The Taper ratio defines the root chord

$$c_{r,H} = \frac{2 \cdot b_H}{A_H \cdot (1 + \lambda_H)} \quad (3.9)$$

$$c_{r,H} = \frac{2 \cdot b_H}{A_H \cdot (1 + \lambda_H)} \quad (3.10)$$

And the tip chord

$$c_{t,H} = \lambda_H \cdot c_{r,H} \quad (3.11)$$

$$c_{t,V} = \lambda_V \cdot c_{r,V} \quad (3.12)$$

The mean aerodynamic chord can now be calculated applying equation 1.3 on the vertical and horizontal tail.

$$c_{MAC,H} = \frac{2}{3} \cdot c_{r,H} \cdot \frac{1 + \lambda_H + \lambda_H^2}{1 + \lambda_H} \quad (3.13)$$

$$c_{MAC,V} = \frac{2}{3} \cdot c_{r,V} \cdot \frac{1 + \lambda_V + \lambda_V^2}{1 + \lambda_V} \quad (3.14)$$

And the mean aerodynamic semi-span locations are found by applying equation 1.4.

$$Y_{MAC,H} = \frac{b}{6} \cdot \left( \frac{1 + 2\lambda_H}{1 + \lambda_H} \right) \quad (3.15)$$

$$Y_{MAC,V} = \frac{b}{6} \cdot \left( \frac{1 + 2\lambda_V}{1 + \lambda_V} \right) \quad (3.16)$$

### 3.3.2 Sweep angle and thickness to chord ratio

In order to avoid tail effectiveness due to shock waves, the drag divergence Mach number of the empennage should be 0.05 higher than that of the wing. This determines the trade off between sweep angle and thickness ratio for the empennage and can be estimated using equation 2.3, given by (**Torenbeek 1988**, Equation 7.38). As mach drag divergence number for the empennage we use that of the wing increased with 0.05.

The lift coefficient of the horizontal tail during cruise can be approximated if we know the trim force it has to exert. The lift coefficient of the vertical tail during cruise flight is zero.

The sweep angle  $\Lambda_{25}$  of the horizontal tail is generally slightly ( $5^\circ$  according to **Scholz 1999**) higher than the wing sweep angle of the wing. This has also the advantage of postponing the stall of the horizontal tail till after the wing stall.

Initial values for both vertical and horizontal tail can be found in Table 3.4 to Table 3.6.

### 3.4 Airfoil selection

The function of the empennage is to stabilize the aircraft, the forces needed to do this during cruise flight are relatively low, in other words, the empennage's produced lift forces stay rather small most of the time. But as they contribute to the wetted area of the aircraft, they contribute to the total drag. The two latter considerations have great influence upon the airfoil selection for the empennage.

In general we can say that an airfoil for the horizontal and vertical tail should be based upon two main airfoil characteristics:

- Being a symmetric airfoil (or slightly negative cambered for horizontal tail)
- Having a low base drag coefficient.

In the tool, the airfoil selection can also be done out of the same library as described in paragraph 2.4.2. In Figure 3.5 the geometry and airfoil selection as described in paragraph 3.3 and 3.4 can be seen as it is integrated in the tool. this is done exactly the same for vertical and horizontal tail so only the horizontal tail is presented.

### 1 horizontal tail geometry

regional turboprop

<b>Aspect Ratio</b>	$A_H$	<input type="text" value="4.91"/> [-]	<b>span horizontal tail</b>	$b_H$	<input type="text" value="13.22"/> [m]
↑	Scholz	<input type="text" value="4.91"/>			
↑	Roskam II	<input type="text" value="3.4 - 7.7"/> [-]			
<b>Sweep</b>	$\Lambda_H$	<input type="text" value="35.00"/> [°]	<b>sweep LE</b>	$\Lambda_{LE}$	<input type="text" value="38.22"/> [°]
↑	Scholz	<input type="text" value="35.00"/> [°]	<b>sweep 50%c</b>	$\Lambda_{50}$	<input type="text" value="31.50"/> [°]
↑	Roskam II	<input type="text" value="0 - 35"/> [°]	<b>sweep TE</b>	$\Lambda_{TE}$	<input type="text" value="23.66"/> [°]
<b>Cruise lift coefficient Horiz</b>	$C_{L,C,H}$	<input type="text" value="0.40"/> [-]		$M_{DDefH}$	<input type="text" value="0.81"/> [-]
<b>thickness ratio</b>	t/c	<input type="text" value="0.08"/> [-]			
↑	torenbeek	t/c <input type="text" value="0.084"/> [-]			
		$k_{m,H}$ <input type="text" value="1.15"/> [-]			
↑	scholz	<input type="text" value="0.088"/>			

Select horizontal tail airfoil

NACA 63-209

**airfoil**

<b>Taper Ratio</b>	$\lambda_H$	<input type="text" value="0.40"/> [-]	<b>root chord horiz</b>	$c_{rH}$	<input type="text" value="3.85"/> [m]
↑	Roskam II	<input type="text" value="0.39 - 1.0"/> [-]	<b>tip chord horiz</b>	$c_{tH}$	<input type="text" value="1.54"/> [m]
<b>dihedral</b>	$\Gamma_H$	<input type="text" value="0.00"/> [°]	<b>Mean aerod chord</b>	$c_{MAC,H}$	<input type="text" value="2.86"/> [m]
↑	Roskam II	<input type="text" value="0 - 12"/> [°]	<b>horiz MAC span</b>	$Y_{MAC,H}$	<input type="text" value="2.83"/> [m]
<b>incidence</b>	$i_H$	<input type="text" value="0.00"/> [°]			
↑	Roskam II	<input type="text" value="0 - 3 fix/variable"/> [°]			

Figure 3.5 Geometry selection of the horizontal tail (idem for vertical tail).

## 3.5 Empennage control surfaces - elevator and rudder

### 3.5.1 Elevator

The elevator is basically a plain trailing edge flap on the horizontal tail, which is designed to make symmetrical deflections (both up- and downward), in order to change the lifting force of the horizontal tail around the center of gravity thus giving pitch control over the aircraft.

The elevator usually extends from the fuselage up to 90% of the span and takes 25 to 35% of the chord. The chord-wise distribution of the elevator can be seen in Table 3.7 for different types of aircraft. The elevator is usually tapered so that it maintains a constant percent chord over its entire span.

The geometry of the elevator can be described using three dimensionless parameters:

- elevator chord distribution  $c_E/c$
- elevator tip chord span  $Y_{r,E}/b_H$
- elevator root chord span  $Y_{t,E}/b_H$

Guidelines can be seen in Table 3.7.

**Table 3.7** Elevator chord and span guidelines (Raymer 2006, p.125)

Aircraft type	$c_E/c$	$Y_{t,E}/b_H$	$Y_{r,E}/b_H$
Business jet	0.32 <sup>a</sup>	0	0.45
Jet Transport	0.25 <sup>a</sup>	0	0.45

<sup>a</sup> often all moving plus elevator.

Once these are selected, different geometric properties of the empennage can be calculated. First we calculate the effective elevator span:

$$Y_{r,E} = \left( \frac{Y_{r,E}}{b_H} \right) \cdot b_H \quad (3.17)$$

First the tip and root chord span of the elevator are calculated with following equations.

$$Y_{r,E} = \left( \frac{Y_{r,E}}{b_H} \right) \cdot b_H \quad (3.18)$$

$$Y_{t,E} = \left( \frac{Y_{t,E}}{b_H} \right) \cdot b_H \quad (3.19)$$

The total elevator root chord and tip chord are the chords of the entire horizontal tail at the elevator tip and root. The effective elevator tip and root chord can then easily be calculated by

multiplying with elevator chord distribution. The total rudder root and tip chord are found using next equations.

$$c_{r,E} = c_{r,H} \cdot \left( 1 - \frac{1 - \lambda_H}{b_H / 2} \cdot Y_{r,E} \right) \quad (3.20)$$

$$c_{t,E} = c_{r,H} \cdot \left( 1 - \frac{1 - \lambda_H}{b_H / 2} \cdot Y_{t,E} \right) \quad (3.21)$$

Now we can calculate the elevator area out of the previously derived geometry.

$$S_E = \frac{b_E}{2} \cdot \left( c_{r,E} \cdot \left( \frac{c_E}{c} \right) + c_{t,E} \cdot \left( \frac{c_E}{c} \right) \right) \quad (3.22)$$

elevator			
select aircraft type			
Jet Transport			
chordwise distribution	$c_E/c$	<input type="text" value="0.25"/>	Total elevator area
↑	Raymer	<input type="text" value="0.25"/>	$S_E$ <input type="text" value="7.13"/> [m <sup>2</sup> ]
elevator root chord span	$Y_{r,E}/b_H$	<input type="text" value="0.05"/>	Total elevator span
↑	Raymer	<input type="text" value="0.05"/>	$b_E$ <input type="text" value="10.58"/> [m]
elevator tip chord span	$Y_{t,E}/b_H$	<input type="text" value="0.45"/>	Elevator root span
↑	Raymer	<input type="text" value="0.45"/>	$Y_{r,E}$ <input type="text" value="0.66"/> [m]
			Elevator tip span
			$Y_{t,E}$ <input type="text" value="5.95"/> [m]
			total Elevator root chord
			$c_{r,E}$ <input type="text" value="3.62"/> [m]
			total Elevator tip chord
			$c_{t,E}$ <input type="text" value="1.77"/> [m]

**Figure 3.6** Elevator geometry selection integrated in tool.

In Figure 3.6 the geometry selection for the elevator is presented. The input required is to set the initial elevator geometry. The guidelines will give “-“ if in there is chosen for an all moving horizontal tail.

### 3.5.2 Rudder

The rudder can be seen as a plain trailing edge flap on the vertical tail, which is designed to make symmetrical deflections (both left- and rightward), in order to change the lifting force of the vertical tail around the center of gravity thus giving yaw control over the aircraft.

The rudder usually extends from the fuselage up to 90% of the span and takes 25 to 35% of the chord. The chord-wise distribution of the rudder can be seen in Table 3.8 for different types of aircraft. The rudder is usually tapered so that it maintains a constant percent chord over its entire span.



The geometric calculations regarding the rudder are quite alike those of the elevator, but some equations are different because the rudder has usually has two symmetric trapezoids whereas the rudder has only one. The geometry of the rudder can be described using three dimensionless parameters:

- rudder chord distribution  $c_R/c$
- rudder tip chord span  $Y_{r,R}/b_V$
- rudder root chord span  $Y_{t,R}/b_V$

Guidelines can be seen in **Table 3.8**

**Table 3.8** Rudder chord and span guidelines (**Raymer 2006**, p124-125)

Aircraft Type	$c_R/c$	$Y_{t,R}/b_V$	$Y_{r,R}/b_V$
Business jet	0.30	0	0.90
Jet Transport	0.32	0	0.90

Once these are selected, different geometric properties of the empennage can be calculated. First we calculate the effective rudder span:

$$Y_{r,R} = \left( \frac{Y_{r,R}}{b_H} \right) \cdot b_H \quad (3.23)$$

First the tip and root chord span of the rudder are calculated with following equations.

$$Y_{r,R} = \left( \frac{Y_{r,R}}{b_V} \right) \cdot b_V \quad (3.24)$$

$$Y_{t,R} = \left( \frac{Y_{t,R}}{b_V} \right) \cdot b_V \quad (3.25)$$

The total rudder root chord and tip chord are the chords of the entire vertical tail at the elevator tip and root. The effective rudder tip and root chord can then easily be calculated by multiplying with rudder chord distribution. The total rudder root and tip chord are found using next equations.

$$c_{r,R} = c_{r,R} \cdot \left( 1 - \frac{1 - \lambda_V}{b_V} \cdot Y_{r,R} \right) \quad (3.26)$$

$$c_{t,R} = c_{r,R} \cdot \left( 1 - \frac{1 - \lambda_V}{b_V} \cdot Y_{t,R} \right) \quad (3.27)$$

Now we can calculate the rudder area out of the previously derived geometry.

$$S_R = \frac{b_R}{2} \cdot \left( c_{r,R} \cdot \left( \frac{c_R}{c} \right) + c_{t,R} \cdot \left( \frac{c_R}{c} \right) \right) \quad (3.28)$$




6 rudder			
chordwise distribution	$c_r/c$ <input type="text" value="0.32"/>	Total Rudder area	$S_R$ <input type="text" value="6.95"/> [m <sup>2</sup> ]
 Raymer	<input type="text" value="0.32"/>	Total Rudder span	$b_R$ <input type="text" value="4.75"/> [m]
elevator root chord span	$Y_{r,R}/b_V$ <input type="text" value="0.10"/>	Rudder root span	$Y_{r,R}$ <input type="text" value="0.59"/> [m]
 Raymer	<input type="text" value="0.10"/>	Rudder tip span	$Y_{t,R}$ <input type="text" value="5.35"/> [m]
elevator tip chord span	$Y_{t,R}/b_V$ <input type="text" value="0.90"/>	total Rudder root chord	$c_{r,R}$ <input type="text" value="5.79"/> [m]
 Raymer	<input type="text" value="0.90"/>	total Rudder tip chord	$c_{t,R}$ <input type="text" value="3.35"/> [m]

Figure 3.7 Rudder geometry selection as integrated in the tool.

In Figure 3.7 the geometry selection for the elevator is presented. The input required is to set the initial elevator geometry. The guidelines will give “-“ if in there is chosen for an all moving horizontal tail.

## 3.6 Tail placement

The location of the empennage with respect to the wing has already been selected, but the location of the vertical and horizontal tail with respect to each other has not been assigned yet. This is called the tail placement, and has some important effect on stall and spin recovery which are herein briefly discussed.

### 3.6.1 Engine slipstream

It is generally not advised to place the horizontal tail directly in the propeller slipstream because of two reasons (**Roskam II 1985**)

- The slipstream causes the tail to buffet, which can lead to excessive cabin noise and early material fatigue of the horizontal tail.
- Rapid engine power changes can lead to undesirably high trim changes.

### 3.6.2 Stall control

If the horizontal stabilizer is in the wake of the wing at the stall angle of attack,  $\alpha_s$ , elevator control will be lost, and further pitch-up may occur. This problem can be avoided by placing the horizontal stabilizer in two possible locations with respect to the wing:

- In line with the mean chord of the wing
- Above the wake of the main wing at the stall angle

These “safe locations” of horizontal tail can be seen on Figure 3.8. All the lengths on this figure have been normalized to the  $c_{MAC}$  of the wing, thus they can be used in determining “safe” vertical positions for the horizontal tail.

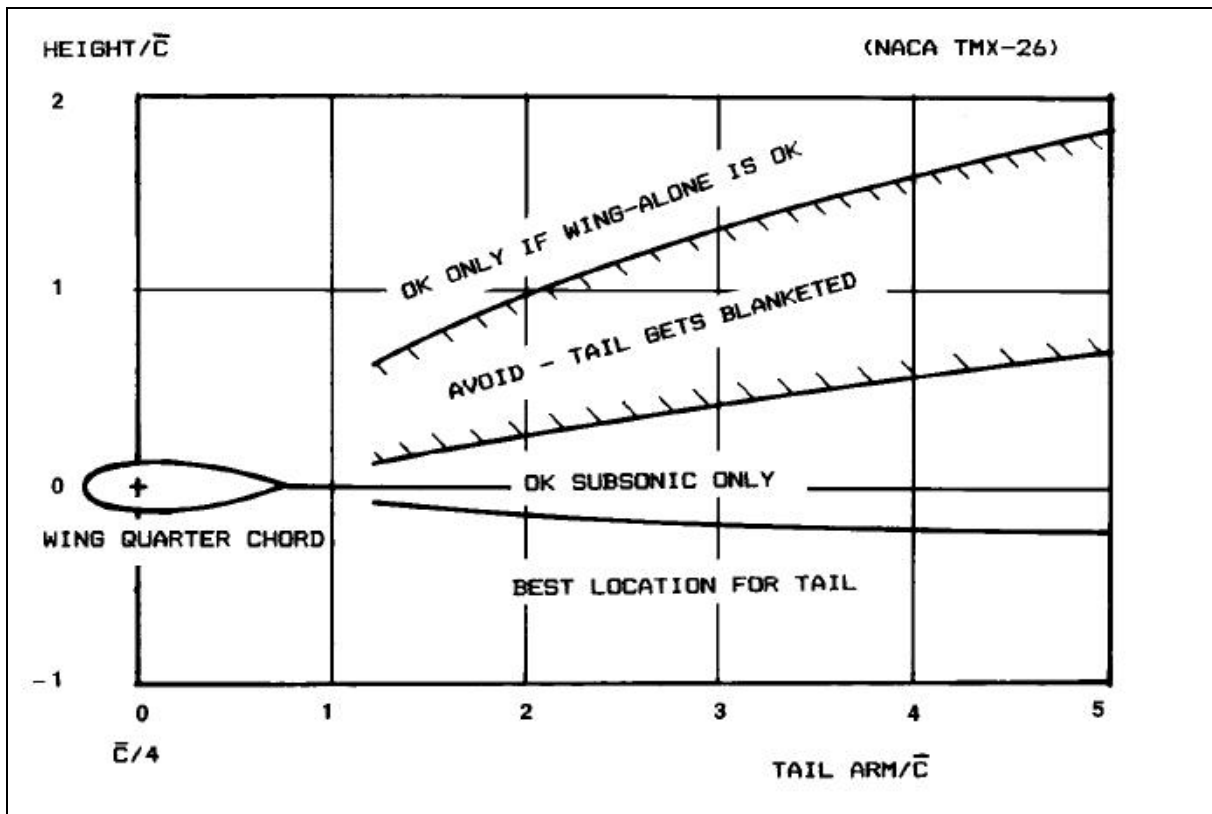


Figure 3.8 Position of the horizontal tail guidelines (Raymer 2006, p.78)

In order to use this method we need to be able to change the vertical position of mean aerodynamic chord of the horizontal tail  $Z_{MAC,H}$ . Since this is geometrically not that useful to work with, we use as input parameter the vertical position of the root chord of the horizontal tail  $Z_{r,H}$ . The relation between the two latter can be given by following equation.

$$Z_{MAC,H} = Z_{r,H} + Y_{MAC,H} \cdot \tan(\Gamma_H) \quad (3.29)$$

The vertical position of the mean aerodynamic chord of the wing is also required and can be found using this equation.

$$Z_{MAC} = Z_r + Y_{MAC} \cdot \tan(\Gamma) \quad (3.30)$$

With  $Z_r$  is the vertical position of the root chord of the wing, which is depending on the vertical wing position (e.g. low wing or high wing ) and the fuselage diameter  $d_f$ . As an approximation we take  $Z_r$  as the most under point (or upper) of the fuselage circle, which results in:

$$\text{For high wing: } Z_r = \frac{d_f}{2} \quad (3.31)$$

$$\text{For low wing: } Z_r = -\frac{d_f}{2} \quad (3.32)$$

The vertical position of the mean aerodynamic chord with respect to the mean aerodynamic chord of the wing is called  $\Delta_{Z,H}$  and can be calculated as follows.

$$\Delta_{Z,H} = Z_{MAC,H} - Z_{MAC} + l_H \cdot \sin \left[ i + \left( \frac{Y_{MAC}}{b/2} \right) \cdot \varepsilon_t \right] \quad (3.33)$$

This formula takes the effect of the incidence angle of the mean aerodynamic chord of the wing into account, because the tail position in Figure 3.8 is defined with respect to the mean aerodynamic chord of the wing, so this equation includes the effect of wing twist and incidence angle.

As horizontal distance between the wing aerodynamic center and the aerodynamic center of the horizontal tail we take the horizontal tail lever arm  $l_H$ , which is actually defined to the center of gravity. But because the CG is still unknown in this phase of the design and because the CG is located near the wing aerodynamic center, this is a good approximation. The effect of incidence angle is also not included, but since the incidence angle is usually small the error is negligible.

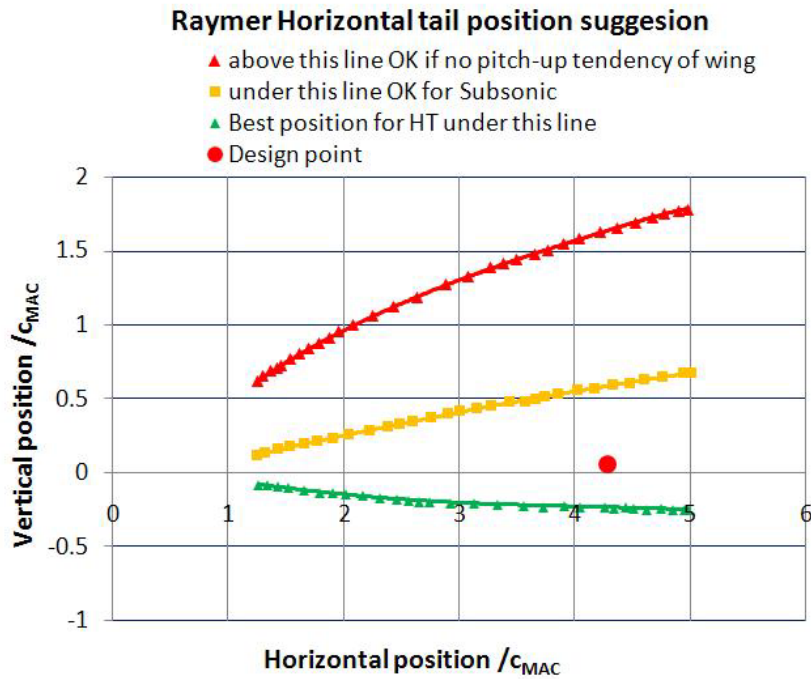


**Figure 3.9** Position of the horizontal tail guidelines as implemented in the Tool.

In order to make the distances ( $l_H$  as horizontal distance and  $\Delta_{Z,H}$  as vertical distance) dimensionless they are divided by the mean aerodynamic chord of the wing. This results in a design point on the diagram seen in Figure 3.9. As the tool is designed for subsonic aircraft, the design point should not be located between the red and yellow border.

### 3.6.3 Spin recovery

The vertical tail plays a key role in the spin recovery, because during a spin the wing is completely stalled and therefore the angle of attack has to be reduced. But if this is done at high angles of sideslip, which occur during a spin, the aircraft immediately enters another spin. Thus in order to reduce the angle of sideslip and the rotation of the aircraft around a vertical axis, rudder control must be maintained. This is only possible if during the spin the rudder stays partially unblanketed by the horizontal tail wake.

Figure 3.10 illustrates the effect of tail arrangement upon rudder control at high angles of attack. The horizontal tail is stalled, producing a turbulent wake extending upward at approximately a  $45^\circ$  angle. The wake borders can be described according to (Raymer 2006, p.83) as a line starting from the leading edge, tilted  $60^\circ$  upward with respect to the chord and a line starting from the trailing edge, tilted  $30^\circ$  upward. In the first case, the rudder lies entirely in the wake of the horizontal tail.

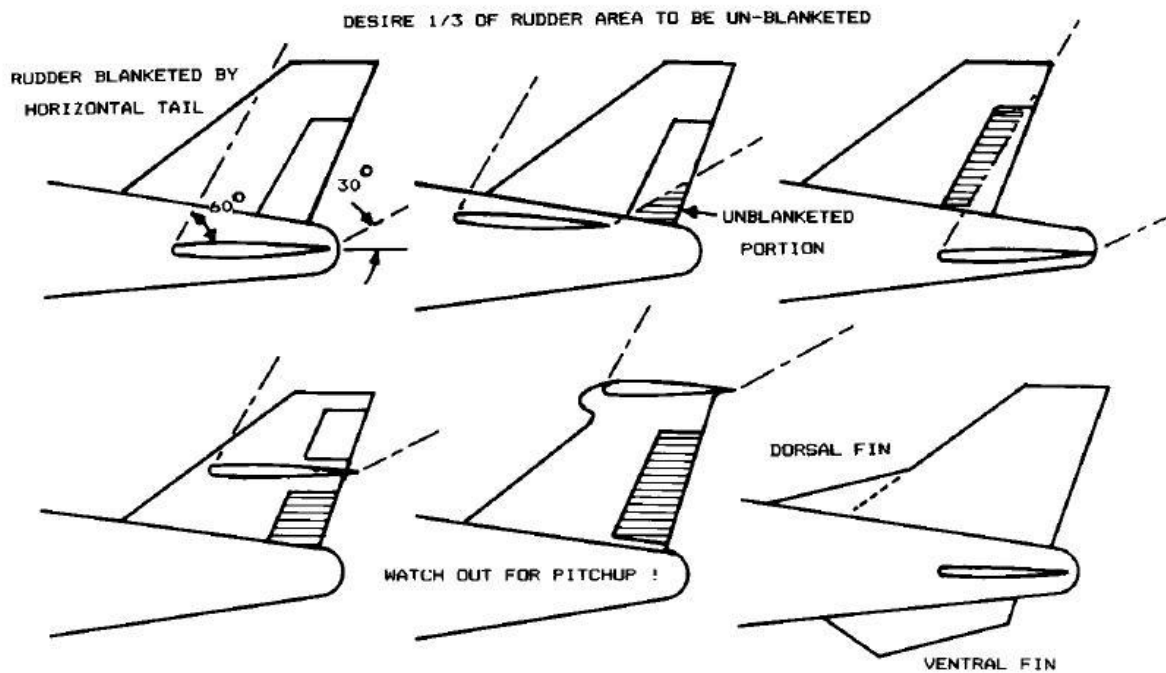


**Figure 3.10** Tail geometry for spin recovery (Raymer 2006, p.83)

As we can see on Figure 3.10, there are several ways of maintaining rudder control:

- Placing the horizontal tail in front or after the rudder, placing the rudder (partially) out of the horizontal tail wake
- Changing the configuration to a T-tail or Cross-Tail, also placing the rudder (partially) out of the horizontal tail wake.
- Using a dorsal fin and/or ventral fins. The dorsal fin improves tail effectiveness at high angles of sideslip, by creating a vortex that attaches to the vertical tail. This prevents high angles of sideslip seen in a spin and improves rudder control. Ventral tails also tend to prevent high angles of sideslip and are placed so that they can never be blanketed by the horizontal tail.

In the first two cases, a good rule of thumb according to (Raymer 2006, p.84) is that 33% of the elevator should stay unblanketed during a spin.

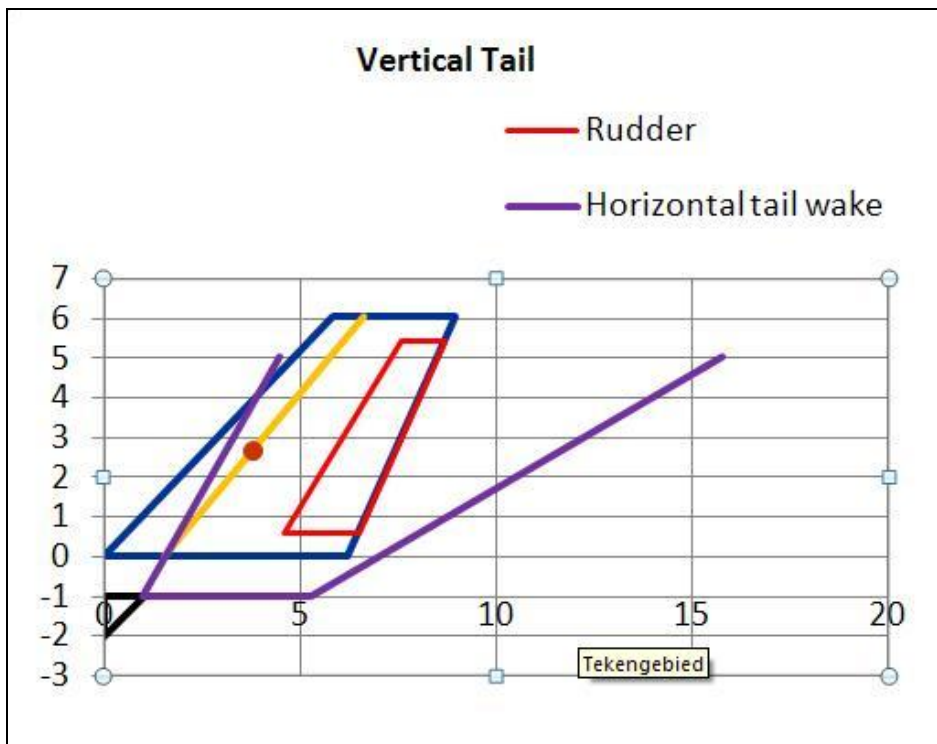


**Figure 3.11** Horizontal tail wake simulated in the tool.

In the tool the vertical tail wake is estimated using previously described approximations as can be seen in Figure 3.11; in this example is clearly visible that the rudder is entirely blanketed by the horizontal tail wake during a spin. The horizontal tail wake is presented by the area above the purple line. The approximation includes the effect of the incidence angle of the horizontal tail.

## Conclusion

The initial goal for the tool setup was to generate input data for PraDO and a general wing and empennage description, based on a minimum of input data. This has been achieved through the use of many guidelines, which can be selected by the user, but certainly don't have to be followed. The user can always use own input data and maintain so enough design autonomy.

If the user applies the guidelines, the wing geometry can be defined almost automatic, since all the guidelines change with the input parameters.

The tool also contains many initial estimates from different authors. This has the advantage that the tool will always give a guideline, which is in many cases an exact value. This makes it easy for the user because there is no range within to select. A problem however arises when two authors strongly disagree. (e.g. aileron suggestions according to Howe and Raymer) Then it becomes difficult for the user to select a value.

Another major advantage of using this tool is that the otherwise time consuming calculations are done automatically, thus resulting in much faster iteration loops. The tool also automatically generates derived geometry data (e.g. MAC, sweep angles...) and the wing geometry is drawn automatically.



## Final remarks

First I would like to say that the tool presented here is one way to deal with the wing and empennage design, it is definitely not the only way

The tool presented here is far from perfect, in that way that there are still some areas where improvement/extension could be done. (These areas were not investigated, or only slightly touched, because they were beyond the scope of the objectives.) To name some examples:

- An extensive airfoil library, with estimations or real test data of lift and drag coefficients could be included.
- An aircraft data library could be integrated, which could be used to select a reference aircraft.
- The 2D and 3D lift calculations could be done more accurate using **(DATCOM 1978)** methods.
- The high lift devices and control surfaces could be designed more accurately using **(DATCOM 1978)** methods.

The problem however with **(DATCOM 1978)** methods is that they include lots of input data, are mainly based on charts, which are not easily to convert into equations. And as the accuracy of **(DATCOM 1978)** methods is also limited, the question rises if it is worth the effort for a few percent of accuracy increase, since this is still the “inaccurate” conceptual design phase.

## **Acknowledgements**

First I would like to thank my parents who made it possible for me to study abroad and supported me in every way they could.

I would also like to thank my supervisor Kolja Seeckt who was always answering my questions and providing me with clear insights in the matters. Further thanks to Prof. Dr. Scholz, who invites students from all over the world to study at the HAW.

And last but definitely not least I would like to thank my friends who always supported me!

## References

- Raymer 2006** RAYMER, Daniel P.: *Aircraft Design: A Conceptual Approach*, Virginia : AIAA, 2006
- Howe 2000** HOWE, D.: *Aircraft Conceptual Design Synthesis*. London : Professional Publishing, 2000
- Jenkinson 1999** JENKINSON, LOYD R., SIMPKIN P, RHODES D.: *Civil Jet Aircraft Design*. London : Arnold, 1999
- Torenbeek 1988** TORENBEEK, E.: *Synthesis of Subsonic Airplane Design*, Delft : Delft University Press, 1988
- Abbott 1959** ABBOTT, I.H.; DOENHOFF, A.E.: *Theory of Wing Sections*, New York : Dover, 1959
- Roskam 1989** ROSKAM, J.: *Airplane Design. Part II : Preliminary Configuration Design and Integration of the Propulsion System*, Ottawa, Kansas, 1989
- DATCOM 1978** HOAK, D.E.: *USAF Stability and Control Datcom*, Wright-Patterson Air Force Base, Air Force Flight Dynamics Laboratory, Flight Control Division, Ohio, 1978. NTIS
- Loftin 1980** LOFTIN, L.K.: *Subsonic Aircraft: Evolution and the Matching of size to Performance*, NASA Reference Publication 1060, 1980
- LAMBERT 1997** LAMBERT, M.: *Jane's all the World's Aircraft*, 1997. - Erscheint jährlich, Jane's Information Group, 163 Brighton Road, Couldsdon, Surrey R5 2NH, UK
- Ciornei 2005** CIORNEI, S.: *Mach number, relative thickness, sweep and lift coefficient of the wing - An empirical investigation of parameters and equations*, unpublished project report, HAW Hamburg, 2005
- Böttger 2004** BÖTTGER O.: *Flügelentwurf - Auslegung der Hauptparameter*, Flugzeugentwurf, HAW Hamburg, 2004
- Scholz 1999** SCHOLZ D.: *Flugzeugentwurf*, Flugzeugentwurf Lecturenotes, HAW Hamburg, 1999

## Appendix A

### Source code of airfoil input macro

```
Private Sub AddFileButton_Click()
    'opens the file select menu
    newfn = Application.GetOpenFilename(FileFilter:="dat files (*.dat), *.dat", Title:="Please select a file")
    If newfn = False Then
        ' They pressed Cancel
        MsgBox "Stopping because you did not select a file"
    Exit Sub
    Else
        Range("A1").Select
        path = "Text;" + newfn
        GetText (path)
    End If
End Sub
```

```
Private Function DeleteTemporary()
    'delete temporary data in colums A to J
    Columns("A:J").Select
    Selection.ClearContents
End Function
```

```
Function GetText(path As String)
    'getting text file in excell sheet
    With ActiveSheet.QueryTables.Add(Connection:=path, Destination:=Range("$A$2"))
        .Name = "goe114"
        .FieldNames = True
        .RowNumbers = False
        .FillAdjacentFormulas = False
        .PreserveFormatting = True
        .RefreshOnFileOpen = False
        .RefreshStyle = xlInsertDeleteCells
        .SavePassword = False
        .SaveData = True
        .AdjustColumnWidth = True
        .RefreshPeriod = 0
        .TextFilePromptOnRefresh = False
        .TextFilePlatform = 850
        .TextFileStartRow = 1
        .TextFileParseType = xlDelimited
        .TextFileTextQualifier = xlTextQualifierDoubleQuote
        .TextFileConsecutiveDelimiter = True
        .TextFileTabDelimiter = True
    End With
End Function
```

```

.TextFileSemicolonDelimiter = False
.TextFileCommaDelimiter = False
.TextFileSpaceDelimiter = True
.TextFileColumnDataTypes = Array(1, 1, 1, 1, 1)
.TextFileTrailingMinusNumbers = True
.Refresh BackgroundQuery:=True
End With

Range("A1").Select
ActiveCell.FormulaR1C1 = "=R[1]C&"" ""&R[1]C[1]&"" ""&R[1]C[2]&"" ""&R[1]C[3]&""
""&R[1]C[4]&"" ""&R[1]C[5]&"" ""&R[1]C[6]&"" ""&R[1]C[7]&"" ""&R[1]C[8]&""
""&R[1]C[9]""

'copy airfoil name to data field (column k to end)
Columns("L:M").Select
Selection.Insert Shift:=xlToRight, CopyOrigin:=xlFormatFromLeftOrAbove
Range("A1").Select
Selection.Copy
Range("L1").Select
Selection.PasteSpecial Paste:=xlPasteValues, Operation:=xlNone, SkipBlanks:=False,
Transpose:=False

'add airfoil name in colum k
Range("K1").Select
Selection.Insert Shift:=xlDown, CopyOrigin:=xlFormatFromLeftOrAbove
Range("A1").Select
Selection.Copy
Range("K1").Select
Selection.PasteSpecial Paste:=xlPasteValues, Operation:=xlNone, SkipBlanks:=False,
Transpose:=False

If Range("A9") = "" Then

    Columns("A:A").Select
    Selection.Delete Shift:=xlToLeft
    Columns("J:J").Select
    Selection.Insert Shift:=xlToRight, CopyOrigin:=xlFormatFromLeftOrAbove

End If

'copy airfoil data to data field (column k to end)
Range("A3:B1000").Select
Application.CutCopyMode = False
Selection.Copy
Range("L2").PasteSpecial Paste:=xlPasteValues, Operation:=xlNone, Skip-
Blanks:=False, Transpose:=False

DeleteTemporary

```

End Function

```
Private Sub AddFolderButton_Click()
    Dim MyPath As String
    MyPath = SelectFolder("Select Folder", "")
    If Len(MyPath) Then
        Openfolder (MyPath)
    Else
        MsgBox "Cancel was pressed"
    End If
End Sub
```

```
Sub FolderSelection()
    Dim MyPath As String
    MyPath = SelectFolder("Select Folder", "")
    If Len(MyPath) Then
        MsgBox MyPath
    Else
        MsgBox "Cancel was pressed"
    End If
End Sub
```

'Both arguments are optional. The first is the dialog caption and  
'the second is to specify the top-most visible folder in the  
'hierarchy. The default is "My Computer."

```
Function SelectFolder(Optional Title As String, Optional TopFolder _
    As String) As String
    Dim objShell As New Shell32.Shell
    Dim objFolder As Shell32.Folder
```

'If you use 16384 instead of 1 on the next line,  
'files are also displayed

```
    Set objFolder = objShell.BrowseForFolder _
        (0, Title, 1, TopFolder)
    If Not objFolder Is Nothing Then
        SelectFolder = objFolder.Items.Item.path
    End If
End Function
```

```
Private Function Openfolder(directory As String)
```

```
    Dim sFil As String
    Dim sPath As String
    Dim FullPath As String
```

```
sPath = directory 'location of files  
ChDir sPath  
sFil = Dir("*.dat") 'change or add formats
```

```
Do While sFil <> "" 'will start LOOP until all files in folder sPath have been looped  
through Set oWbk = Workbooks.Open(sPath & "\" & sFil) 'opens the file  
FullPath = "Text;" + sPath + "\" + sFil
```

```
'Range("A1") = Dir  
GetText (FullPath)  
sFil = Dir
```

```
Loop ' End of LOOP
```

```
End Function
```

```
Private Sub DeleteButton_Click()  
Rows("1:5000").Select  
Selection.Delete Shift:=xlUp  
Range("A1").Select  
End Sub
```